**Extended Numerical Analysis on Gas Turbine Blade Cooling**

by

WEE TIAT DONG

Dissertation submitted in partial fulfilment of
the requirements for the
Bachelor of Engineering (Hons)
(Mechanical Engineering)

MAY 2011

Universiti Teknologi PETRONAS
Bandar Seri Iskandar
31750 Tronoh
Perak Darul Ridzuan

# CERTIFICATION OF APPROVAL

**Extended Numerical Analysis on Gas Turbine Gas Cooling**

by

WEE TIAT DONG

A project dissertation submitted to the
Mechanical Engineering Programme
Universiti Teknologi PETRONAS
in partial fulfilment of the requirement for the
BACHELOR OF ENGINEERING (Hons)
(MECHANICAL ENGINEERING)

Approved by,

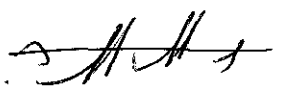

(Assoc. Prof. Dr. Hussain H. Al-Kayiem)

UNIVERSITI TEKNOLOGI PETRONAS

TRONOH, PERAK

May 2011

## CERTIFICATION OF ORIGINALITY

This is to certify that I am responsible for the work submitted in this project, that the original work is my own except as specified in the references and acknowledgements, and that the original work contained herein have not been undertaken or done by unspecified sources or persons.

17/9/2011

WEE TIAT DONG

# ABSTRACT

The main objective of this project is to simulate the Gas Turbine blade cooling by Finite Element using ANSYS-FLUENT software. Using Gambit and Fluent software, the effect of the channel ribbing configuration on the cooling efficiency is investigated. A real gas turbine blade (143MW ABB GT13E2) contributed by Lumut Power plant was used for the studies. The blade was then taken for digitizing to get the real dimension in the form of AutoCad drawing. The drawing was then export to Gambit for further analysis such as meshing and boundary condition setting. Once the setting been done in Gambit, it will then be exported to Fluent for simulation.

Grid Independency is an important issue whereby we will look at the starting size, growth rate and size limit for meshing the blade. A small size and growth rate will result in a large total of element in which in return will give trouble to the simulation.

Flowing into a rectangular 9mm x 18mm channel, the 400K compressed air is used to cool the blade while the blade is spinning in the hot gas of 1700K. The temperature distribution is then compared to the result using analytical method (Matlab) done by previous student. The result shows that the temperature difference is less than 5% for the root of the blade and 15.92% for height of 157.7mm channel.

From the study done by previous student a rib channel with rib angle, $\alpha = 60^{\circ}$ and rib blockage ratio, $e/D_h = 0.078$ will result in largest convection coefficient which is $H_{ribbed} = 559.32\ W/m^2.K$. This parameter of ribbed channel will then be compared with smoothed channel cooling. The result shows that there a decrease in temperature which brings to 8.68% more efficient if using two-opposite rib wall.

# ACKNOWLEDGEMENT

The author would like to express humble gratitude to the author's family, FYP's supervisor, Assoc. Prof. Dr. Hussain H. Al-Kayiem, UTP's technicians, Mr. Zailan and Mr. Irwan, Mr Aja Ogboo Chikere and friends all over. These people have helped the author a lot to successfully complete this project within the time provided. It has been a wonderful time working together and the author has learned a lot in a short period of time.

In the way to become an engineer, it is important for the author to have a positive mind set during this period so as to avoid bad habits such as laziness and procrastination. Throughout the three semesters, the author has gained a valuable experience in various aspects especially in engineering materials. The exposure to such environment will be very useful to the author's future career. The author hope to make good use of the knowledge gained.

It was a great experience and knowledge that the author has gained in term of engineering aspect or software mastering. Even thought there are more detail and advance on using the software, the author was grateful that he has familiar with the basic use on the software.

# TABLE OF CONTENTS

# LIST OF FIGURES

# LIST OF TABLES

# LIST OF APPENDIX

# ABBREVIATION

The following abbreviations are used throughout this document:

| | |
|---|---|
| GT | Gas Turbine |
| CFD | Computational Fluid Dynamics |
| ECD | Electrochemical Drilling |
| IFC | Impingement/Film Cooling |
| RIT | Rotor Inlet Temperature |
| RAM | Random Access Memory |

# CHAPTER 1

# INTRODUCTION

## 1.1 BACKGROUND OF STUDY

Gas Turbine engines are designed to continuously and efficiently convert the energy of fuel into useful power and are developed into very reliable, high performance engines. Now, gas turbines are widely used in power plants, marine industries and aircraft.

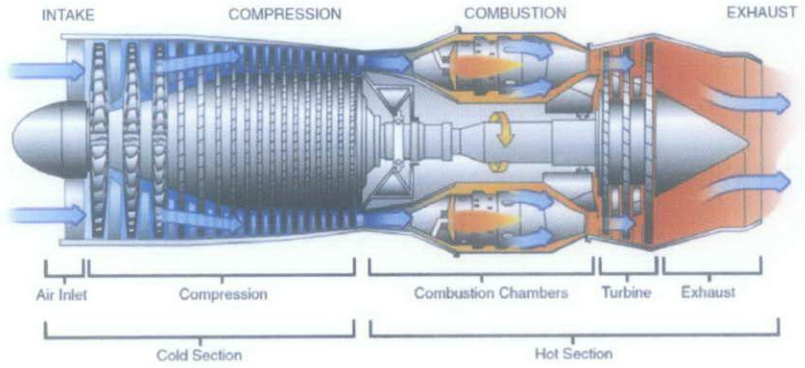


Figure 1.1: Basic Gas Turbine Cycle [FAA 2004 Airplane Flying Handbook]

From the Fig. 1.1, temperature in the hot section of the engine can reach to 3000°F, which is roughly 500°F hotter than the melting temperature of the turbine's airfoils [3]. Starting from early 1970s, many research have been carried out by aircraft and power generation gas turbine designers to increase the combustion chamber exit and high-pressure turbine stage inlet temperatures. By increase the combustion chamber exit temperature, the efficiency can be improved and fuel consumption can be reduced [1].

## 1.2 PROBLEM STATEMENT

Gas Turbine cooling by compressed air has been investigated by previous student in the department. Discretization has been carried out using finite difference and the set of equations has been solved by using matrix inversion. However, only the first quarter of the blade was covered in the analysis, and there is a need to investigate the entire blade by Finite Elements.

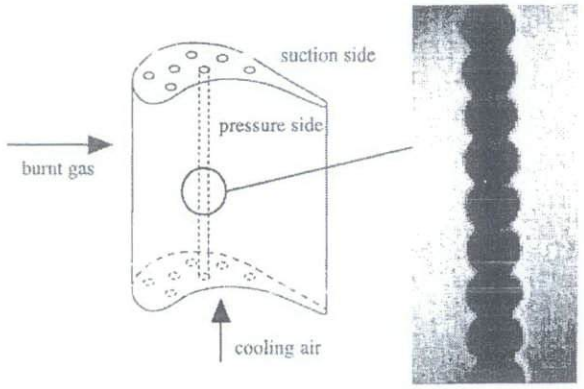


Figure 1.2 : Turbine blade with cooling holes [5]

## 1.3 OBJECTIVES

The main objectives of this project are :-

- To simulate the Gas Turbine blade cooling by Finite Element using ANSYS-FLUENT software and;
- To investigate the effect of the channel ribbing configuration on the cooling efficiency.

## 1.4 SCOPE OF STUDY

A Gas Turbine blade with internal cooling was selected for previous numerical analysis. In the present work, the blade is to be simulated by finite element/finite volume to study the cooling at various floe rates, various channels and various cooling technique like the film cooling.

In this project, Auto CAD will be used for modelling purpose. Modelling process is important because when the dimension is accurate, better result can be obtained. After the modelling is done, ANSYS-FLUENT will be used for simulation. For the simulation, there are certain parameters that should be followed or used as it is the requirements for the simulation.

This project covers the simulation of the smooth hole of the channel of cooling blade and also the ribbed channel with specific angle. The ribbed angle that will be used for simulation is chosen from the previous study that been done that would be $90^{o}$, $60^{o}$, and $45^{o}$. Through the simulation, fixtures such as temperature, pressure and heat distribution can be seen clearly. From the simulation result, we can know which factor affect the cooling system most, and hence the efficiency of the Gas Turbine cooling blade can be increased and improved.

# CHAPTER 2

# LITERATURE REVIEW & THEORY

This chapter will review on the research that have been done in the past and will be used as reference.

## 2.1 THEORY

The main purpose of this study is to increase the efficiency of the gas turbine. In order to do so, it is crucial to maximise the adiabatic effectiveness (film effectiveness). The parameter is dependent upon the three temperatures, that are the mainstream, coolant, and the surface being cooled; which is defined as:-

$$\xi = \frac{T_{aw} - T_m}{T_c - T_m}$$

Adiabatic effectiveness measures the efficiency of a coolant film in which a value of unity indicates that the temperature of the surface being cooled is equal to the coolant temperature. Heat transfer coefficients play an important role in determining the effectiveness of film cooling. In order to meet the objective of film cooling, a low heat transfer coefficient should be achieved from the surrounding hot mainstream to the surface as well as a large effectiveness on the surface. The results are as below:-

$$\frac{h_1}{h_0} = \left(\frac{q_1}{q_0}\right)\left(\frac{T_m - T_w}{T_{aw} - T_w}\right)$$

Blowing ratio is another parameter that are important in this studies. Density and velocity of the mainstream and coolant flows are the components in this property, which is defined as:-

$$\mathrm{M} = \frac{\rho_c U_c}{\rho_m U_c}$$

The effect of this parameter on the adiabatic effectiveness is the primary interest for a number of studies due to its significant impact on the film cooling performance [1].

## 2.2 COOLING MECHANISM

There are two types of cooling in gas turbine system. The first type is the internal cooling. In this type of cooling, air is bled from the compressor stage and then passed through internal passages incorporated into blade designs (Fig. 2.1). This method is known as enhanced passage cooling because it is the most common technique. In order to maximise the heat absorption, the air is allowed to impinge on the internal wall of the blade. This technique is called impingement cooling [1].

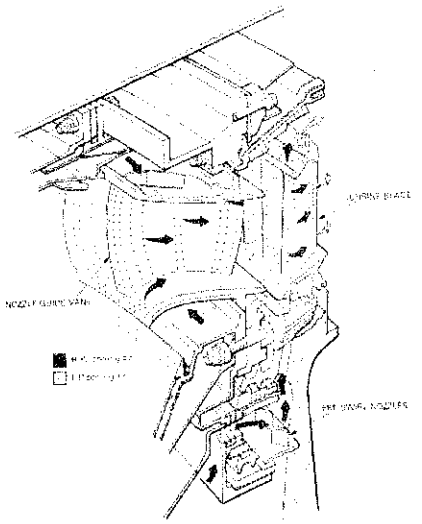

Figure 2.1: Cooling air flow in a high pressure turbine [9]

Second type of cooling is known as external cooling. Air is bled from the compressor stage, ducted through the internal chambers of the turbine blades, and then discharged through small holes/slots on the blade outer walls. This air provides a thin, cooler, insulating film along the external surface of the turbine, due to which the method is called "film cooling". As a result, the film provides protection and thus increases the life of the blade. If the blade's operating temperature was off the maximum design temperature by 50°F (10°C), then the life of the blade maybe reduced by 50% [1].

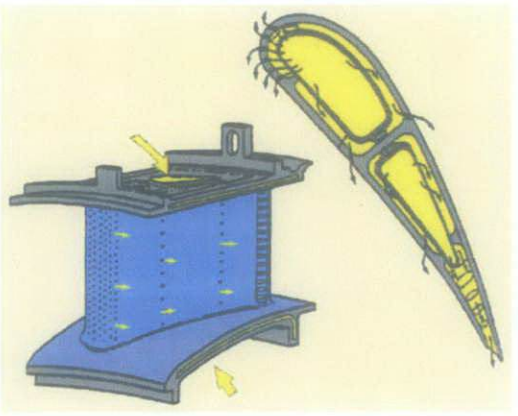

Figure 2.2: Film cooling of turbine blades in Gas Turbines [8]

## 2.3 CHANNEL WALL CONFIGURATION

The temperature distribution of compressed air can be categorised into two different cooling channel configurations. In the first type, we have this so called smooth due to the non-ribbed channel wall. Meanwhile, for the second type, the channel walls are artificially roughened by regular repeated ribs (Fig.2.3).

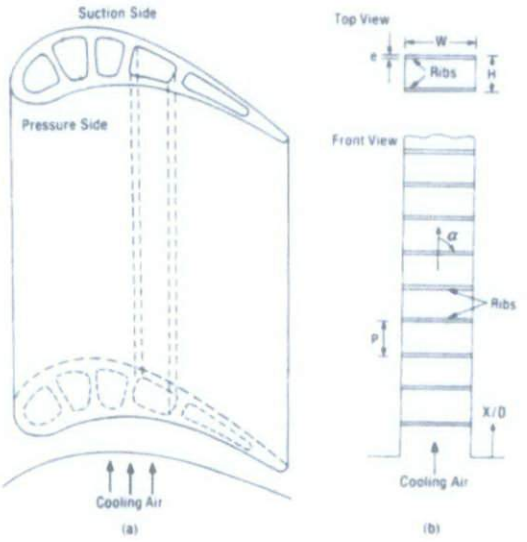


Figure 2.3: Typical coolant channels in turbine airfoils and internal rib arrangement [7]

## 2.4 COOLING TECHNOLOGY

As mention in section 2.2, the cooling technology can be divided into two that are internal and external cooling. In order to increase the heat transfer from turbine blade to the coolant air, different technologies were used [6]:-

1. Rib

   The function is to trip the boundary layer directly after it has been attached. By this, the turbulence and heat transfer will be increased. The rib can be V-format or in combination of matrix. Still, lots of studies are needed to achieve the optimum maximum heat transfer for minimum pressure losses.

2. Pin-fin and Dimples cooling

   Pins are placed in the channel to create a circulation zone behind and a high heat transfer. Meanwhile, the dimples are used to place holes in the wall to create turbulence, and high heat transfer.

3. Impingement Cooling

   This type of cooling is used when the concentrated airflow is impinging on the inner surface of the blade through some small hole.

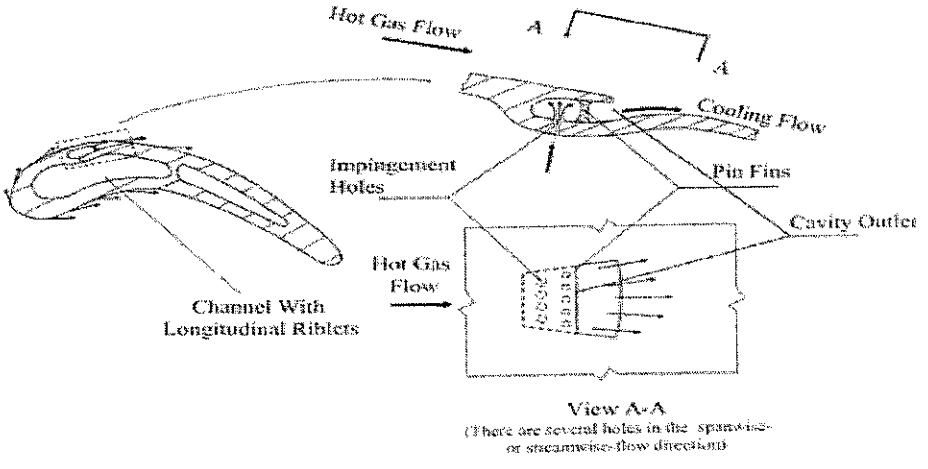


Figure 2.4: Impingement hole, Pin-fins and Firm cooling [6]

## 2.5 RIB-TURBULATED COOLING

According to Han (1984), factors like channel aspect ratio, rib configuration, and flow Reynolds number will affect the heat-transfer performance in a stationary ribbed channel. In general, a typical ribs height that are used for experimental studies are around 5% - 10% of channel hydraulic diameter. *p/e* ratio varying from 7 to 15 [2].

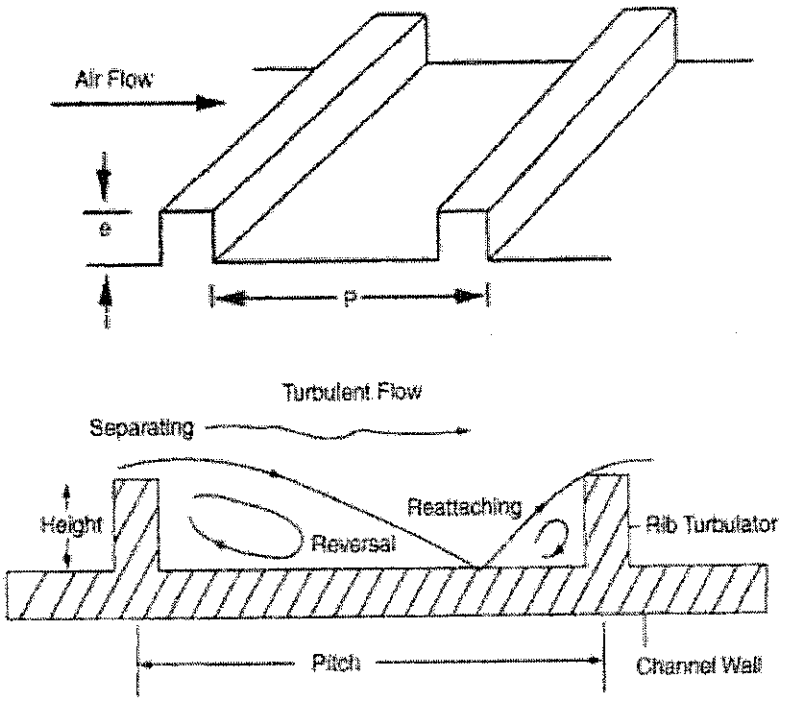


Figure 2.5: Schematic of flow separation and rib orientations in heat-transfer coefficient enhancement (Han and Dutta, 1995) [2]

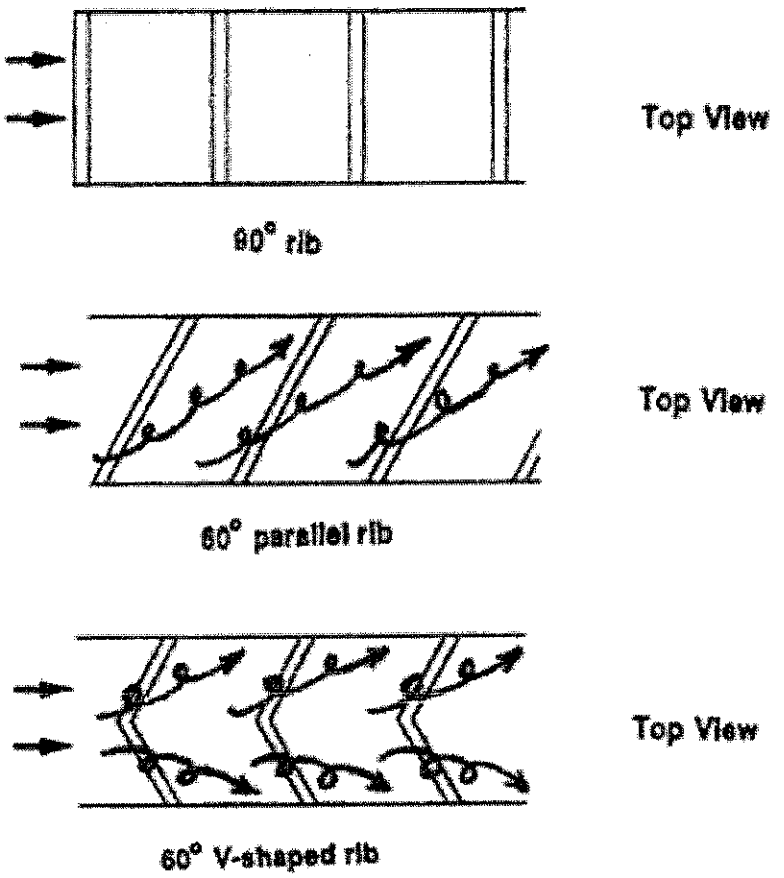


Figure 2.6: Schematic of secondary flow developed along angled-rib orientations (Han and Dutta, 1995) [2]

Figure 2.5 & 2.6 shows the nomenclature geometrical features of ribs that are commonly used. *e* represents rib height; P represent rib-to-rib. Schematic of the flow past surface-mounted ribs is shown in the figure; a boundary layer is separating upstream and downstream of the ribs. Several studies show that another separation region may exist on top of the ribs. Separated boundary layer enhances turbulent mixing and thus dissipates the heat from the near-surface fluid into the main flow. This increases heat-transfer coefficient.

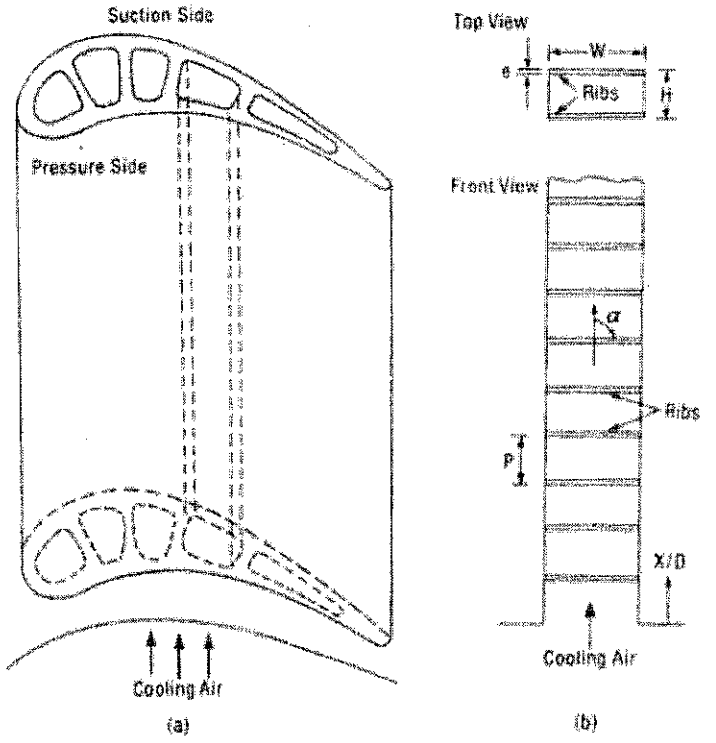


Figure 2.7: Typical coolant channels in turbine airfoil and internal rib arrangement (Han, 1988) [2]

Typical coolant channel orientation in a turbine blade is shown in Figure 2.7. As the result of the curved asymmetric shape of a turbine blade, the cooling channels near the trailing edge have broad aspect ratios, and those near the leading edge have narrow aspect ratios. Usually suction and pressure sides are ribbed. For orthogonal or transverse ribs, the angle of attack $\alpha$ is $90^{\circ}$; other than $90^{\circ}$ is called skewed [2].

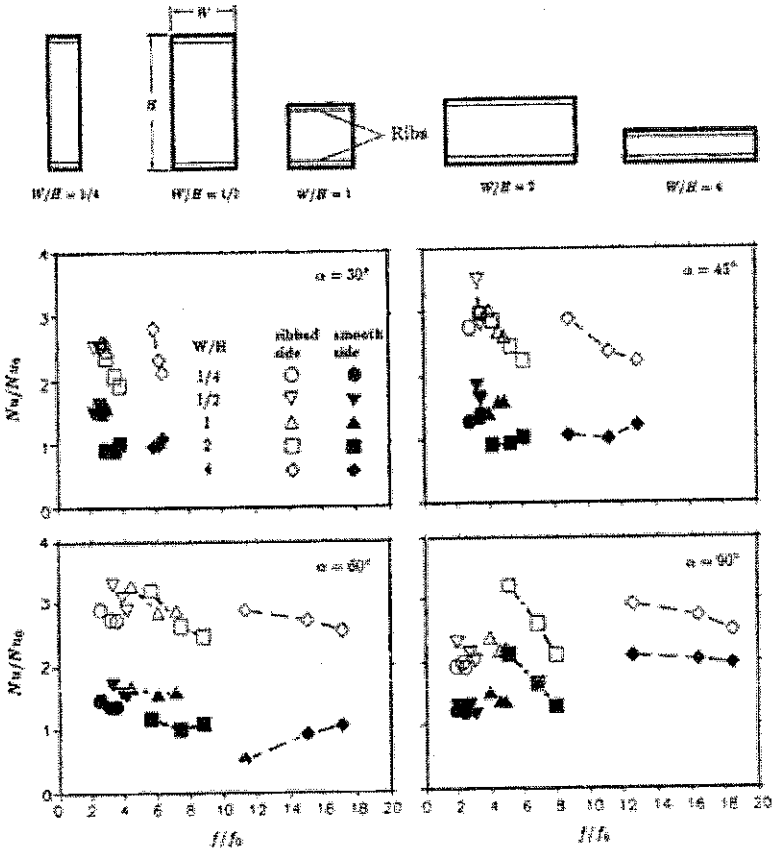


Figure 2.8: Effect of channel aspect ratio on heat-transfer performance (Part et al., 1992) [2]

From Figure 2.8 above, when the channel aspect ratio changes from narrow to wide (1/2 to 4), the ribbed-side heat transfer augmentations for 60° ribs do not vary significantly, but the pressure drop penalties increase dramatically from 2- to 18-fold. Same result is observed for 45° and 90° ribs. Thus, we can say that a narrow-aspect ratio channel provides a better heat-transfer performance than a broad-aspect ratio channel. For 30° ribs, both heat-transfer enhancement and pressure drop increment are relatively low in narrow-aspect ratios. Friction factor is significant low for 30° ribs in a broad-aspect ratio duct (W/H = 4), and the heat-transfer coefficient is comparable to other ribs.

## 2.6 V-SHAPED RIBS

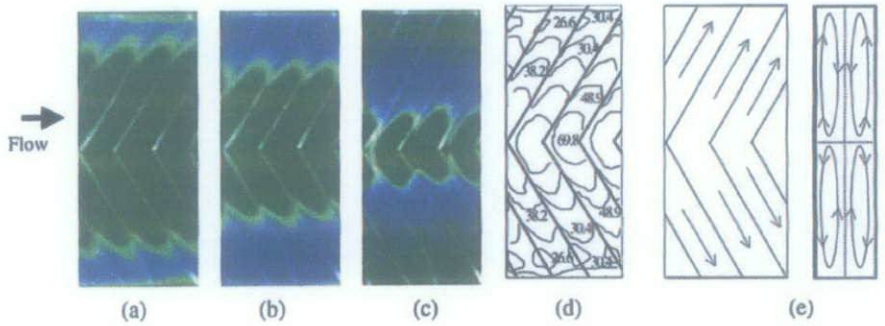


Figure 2.9 V-shaped upstream[10]

Figure 2.9 shows V-shaped ribs pointing upstream compared to the main flow direction at Reynolds number of 6000. **a** $q_w$ = 354 W/m$^2$, **b** = 437 W/m$^2$ , **c** = 660 W/m$^2$ **d** Local Nusselt number contours on the V-rib-roughened surface, **e** Schematic pattern of the secondary flow induced by V-ribs [10]

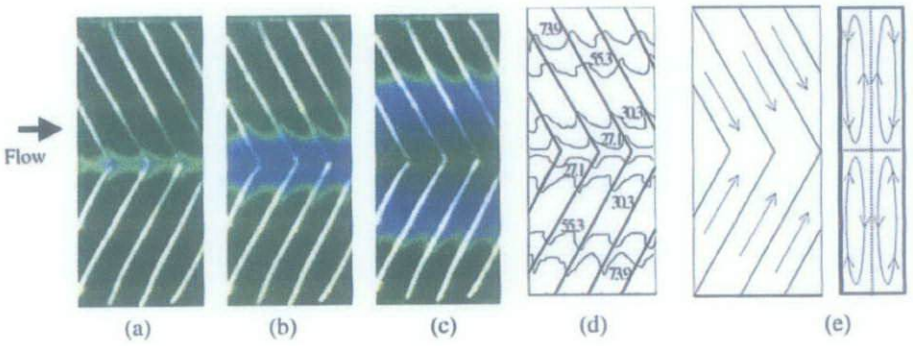


Figure 2.10 V-shaped downstream [10]

Figure 2.10 shows V-shaped ribs pointing downstream of the main flow direction at Reynolds number of 6000. **a** $q_w$ = 383 W/m$^2$, **b** = 455 W/m$^2$ , **c** = 575 W/m$^2$ **d** Local Nusselt number contours on the V-rib-roughened surface, **e** Schematic pattern of the secondary flow induced by V-ribs[10]

The heat transfer coefficient shows a significant spanwise variation in Figure 2.9 & Figure 2.10. For the V-ribs pointing upstream of the main flow direction, the local Nusselt numbers are lowest on both top and bottom sides, while the highest values occur in the central duct area. For the V-ribs pointing downstream of the main flow direction, the heat transfer distribution is opposite, the central apex region has the lowest Nusselt number and the junctions between the ribbed wall and the top and bottom smooth walls have the highest values. This spanwise variation is attributed to different secondary flows induced by the orientations of the angled V-ribs.

# CHAPTER 3

# METHODOLOGY

## 3.1 ANALYSIS TECHNIQUES

Numerical analysis is carried out for the project. This analysis can be done by simulation of finite element using ANSYS-FLUENT software. Although it is simulation, gas turbine information should be gathered to make sure the understanding of the project is enough. Mathematical calculation might be used for the formulae or equations related to the project. Before meshing the model, Auto CAD drawing might be useful to come out with the actual shape.

## 3.2 METHODS/TOOLS

The software that will be used is ANSYS-FLUENT software. It performs various type of simulations based on the parameter given. In this project, finite element or finite volume is simulate according to various flow rates, various channels, and various cooling technique

## 3.3 FLOW CHART

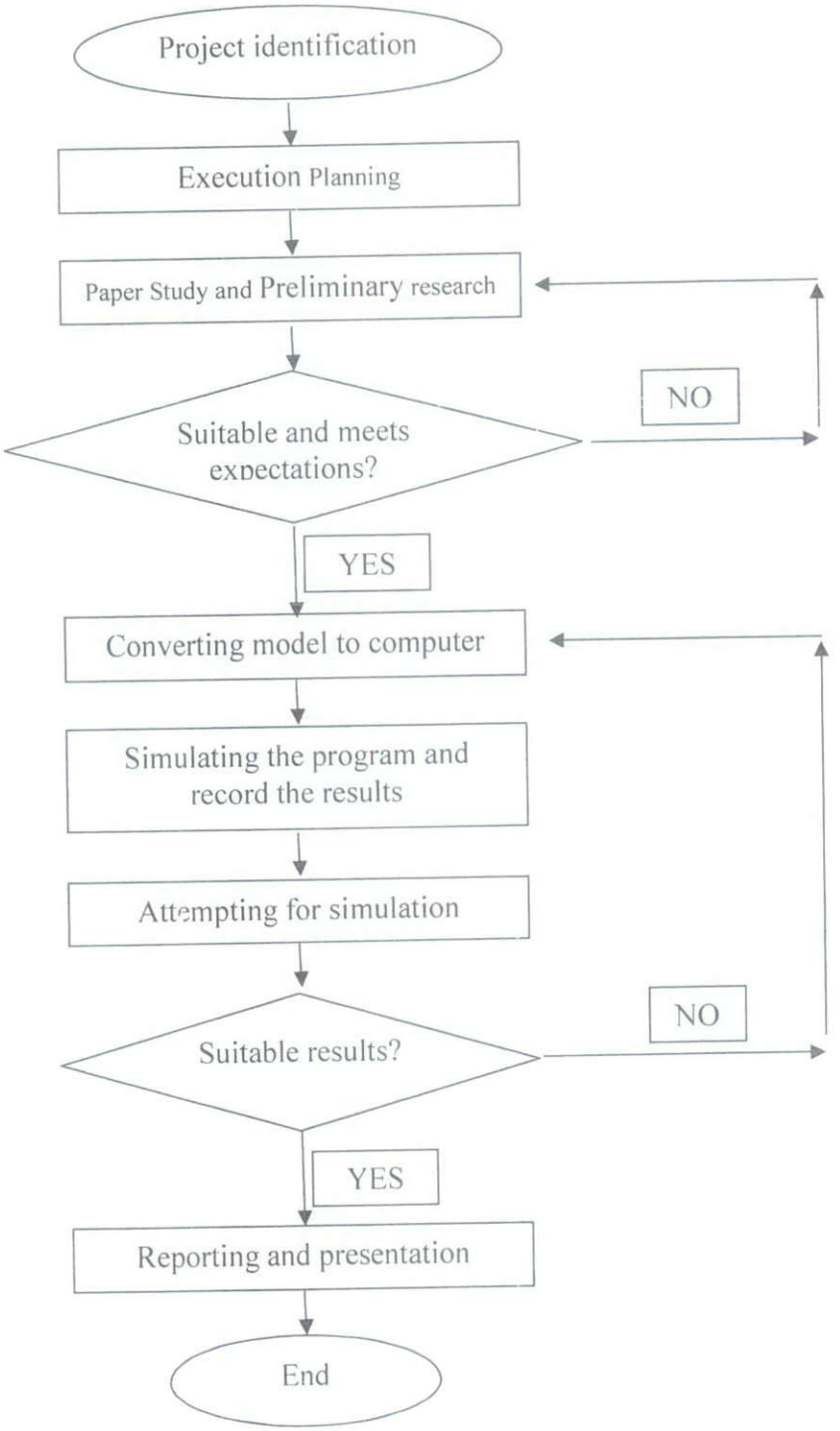

## 3.4 GANTT CHART

FYP I

Sugested Milestone for First Semester Final Year Project (FYP I) - WEE TIAT DONG (ME) 11711

| No. | Detail/Week | 1 | 2 | 3 | 4 | 5 | 6 | | 7 | 8 | 9 | 10 | 11 | 12 | 13 | 14 | SW | EW |
|---|---|---|---|---|---|---|---|---|---|---|---|---|---|---|---|---|---|---|
| 1 | Confirmation of Propose Topic | | | | | | | | | | | | | | | | | |
| | -Submission of Title Proposals | | | | | | | | | | | | | | | | | |
| | -Selection of Title Proposals (Form 01 , Form 02) | | | | | | | | | | | | | | | | | |
| | -Assignment of Titles & SVs | | | | | | | | | | | | | | | | | |
| | -Approved of Titles & SVs | | | | | | | | | | | | | | | | | |
| | | | | | | | | | | | | | | | | | | |
| 2 | Background Study | | | | | | | | | | | | | | | | | |
| | -Search & collect journal/article | | | | | | | | | | | | | | | | | |
| | -Read Amir Hossein's thesis | | | | | | | | | | | | | | | | | |
| | -Project Planning | | | | | | | | | | | | | | | | | |
| | -Submission of preliminary report (20th August 2010) | | | | | | | | | | | | | | | | | |
| | | | | | | | | | | | | | | | | | | |
| 3 | Further understanding | | | | | | | | | | | | | | | | | |
| | -Installing & familiarizing with ANSYS-FLUENT | | | | | | | | | | | | | | | | | |
| | | | | | | | | | | | | | | | | | | |
| 4 | Lab Work | | | | | | | | | | | | | | | | | |
| | -Simulation work by Finite Element using Gambit | | | | | | | | | | | | | | | | | |
| | -Investigation of the effect of channel ribbing configuration | | | | | | | | | | | | | | | | | |
| | | | | | | | | | | | | | | | | | | |
| 5 | Submission of Progress report & Seminar | | | | | | | | | | | | | | | | | |
| 6 | Submission of Interim Report Final Draft (SV) | | | | | | | | | | | | | | | | | |
| 7 | Submission of Interim Report Final Draft (2 copies to Co-ordinator) | | | | | | | | | | | | | | | | | |
| 8 | Submission of Interim Report (3 copies to Co-ordinator & SV) (1st Nov 2010) | | | | | | | | | | | | | | | | | |
| 9 | Oral Presentation | | | | | | | | | | | | | | | | | |

Mid-Semester Break

Required Milestone  Process  Suggested Milestone

## FYP II

Sugested Milestone for First Semester Final Year Project (FYP II) - WEE TIAT DONG (ME) 11711

| No. | Detail/Week | 1 | 2 | 3 | 4 | 5 | 6 | 7 | | 8 | 9 | 10 | 11 | 12 | 13 | 14 | SW | EW |
|---|---|---|---|---|---|---|---|---|---|---|---|---|---|---|---|---|---|---|
| 1 | Lab Work | | | | | | | | | | | | | | | | | |
| | -Simulation work by Finite Element using Gambit | | | | | | | | | | | | | | | | | |
| | -Investigation of the effect of channel ribbing configuration | | | | | | | | | | | | | | | | | |
| | | | | | | | | | | | | | | | | | | |
| 2 | Submission of Progress Report I | | | | | | | | | | | | | | | | | |
| | | | | | | | | | | | | | | | | | | |
| 3 | Project/Lab work continues | | | | | | | | | | | | | | | | | |
| | | | | | | | | | | | | | | | | | | |
| 4 | Submission of Progress Report II | | | | | | | | | | | | | | | | | |
| | | | | | | | | | | | | | | | | | | |
| 5 | Seminar (compulsory) | | | | | | | | | | | | | | | | | |
| | | | | | | | | | | | | | | | | | | |
| 6 | Project/Lab work continues | | | | | | | | | | | | | | | | | |
| | | | | | | | | | | | | | | | | | | |
| 7 | Poster Exibition | | | | | | | | | | | | | | | | | |
| | | | | | | | | | | | | | | | | | | |
| 8 | Submission of Dissertation Report Final Draft (SV) | | | | | | | | | | | | | | | | | |
| 9 | Submission of Dissertation Report Final Draft (2 copies to Co-ordinator) | | | | | | | | | | | | | | | | | |
| 10 | Submission of Dissertation Report (3 copies to Co-ordinator & SV) | | | | | | | | | | | | | | | | | |
| 11 | Oral Presentation | | | | | | | | | | | | | | | | | |
| 12 | Submission of Dissertation Report Final Copy (Hardbound) | | | | | | | | | | | | | | | | | |

Mid-Semester Break

Required Milestone  Process  Suggested Milestone

# CHAPTER 4

# RESULTS AND DISCUSSION

## 4.1 GRID INDEPENDENCY

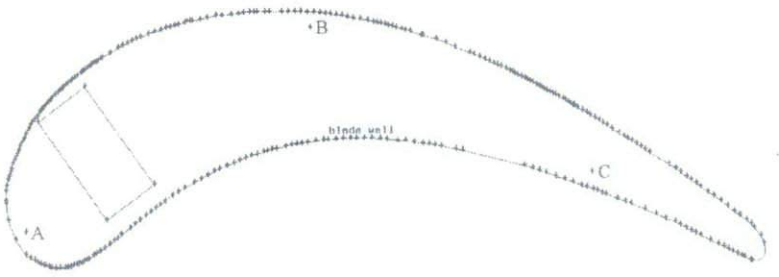


Figure 4.1: Point A, Point B, & Point C

Grid independency is used to check for the lowest total element that the blade can run without affecting much on its temperature reading. This is necessary because if the meshing size is increase, the total element will be reduced and hence reduce the load and time for the simulation.

First we will set the Start Size, Growth Rate, and Size Limit. The variables will keep on changing until the temperature at the three points (point A, point B, and point C) reach a difference of more than 5% (70degree Kelvin difference). The variables also depend on the software itself; if the blade cannot be meshed for a bigger growth rate, then the previous size of growth rate will be chosen. Table below shows the temperature different for different size function.

### 4.1.1 BLADE SIZE FUNCTION

| Size Function | | | Total Element | | Temperature (K) | | |
|---|---|---|---|---|---|---|---|
| Start Size | Growth Rate | Size Limit | Blade | Channel | Point A | Point B | Point C |
| 0.9 | 1 | 0.9 | 560196 | 46800 | 1410.4076 | 1410.4076 | 1410.4076 |
| 0.9 | 1 | 3 | 560196 | 46800 | 1410.4076 | 1410.4076 | 1410.4076 |
| 0.9 | 1 | 6 | 560196 | 46800 | 1410.4076 | 1410.4076 | 1410.4076 |
| 0.9 | 1 | 9 | 560196 | 46800 | 1410.4076 | 1410.4076 | 1410.4076 |
| 0.9 | 1 | 90 | 560196 | 46800 | 1410.4076 | 1410.4076 | 1410.4076 |
| 0.9 | 3 | 0.9 | 560196 | 46800 | 1414.2041 | 1414.2041 | 1414.2041 |
| 0.9 | 3 | 3 | 164736 | 46800 | 1410.4076 | 1410.4076 | 1410.4076 |
| 0.9 | 3 | 4.5 | Error in Meshing | | | | |
| 1.8 | 3 | 3 | 162162 | 46800 | 1386.5411 | 1386.5411 | 1386.5411 |
| 0.9 | 6 | 0.9 | 560196 | 46800 | 1414.2041 | 1414.2041 | 1414.2041 |
| 0.9 | 6 | 3 | Error in Fluent - Diverge | | | | |
| 0.9 | 6 | 6 | Error in Meshing | | | | |
| 0.9 | 6 | 9 | Error in Meshing | | | | |
| 0.9 | 9 | 0.9 | 560196 | 46800 | 1414.2041 | 1414.2041 | 1414.2041 |
| 0.9 | 9 | 3 | 165438 | 46800 | Error in Fluent | | |
| 0.9 | 9 | 6 | Error in Meshing | | | | |
| 0.9 | 9 | 9 | Error in Meshing | | | | |
| 0.9 | 12 | 0.9 | 560196 | 46800 | 1414.2041 | 1414.2041 | 1414.2041 |
| 0.9 | 12 | 3 | 167544 | 46800 | 1414.2041 | 1414.2041 | 1414.2041 |
| 0.9 | 12 | 6 | Error in Meshing | | | | |
| 0.9 | 12 | 9 | Error in Meshing | | | | |

Table 4.1: Size function variable for blade (with same Growth Rate for comparison)

| Size Function | | | Total Element | | Temperature (K) | | |
|---|---|---|---|---|---|---|---|
| Start Size | Growth Rate | Size Limit | Blade | Channel | Point A | Point B | Point C |
| 0.9 | 1 | 0.9 | 560196 | 46800 | 1410.4076 | 1410.4076 | 1410.4076 |
| 0.9 | 3 | 0.9 | 560196 | 46800 | 1414.2041 | 1414.2041 | 1414.2041 |
| 0.9 | 6 | 0.9 | 560196 | 46800 | 1414.2041 | 1414.2041 | 1414.2041 |
| 0.9 | 9 | 0.9 | 560196 | 46800 | 1414.2041 | 1414.2041 | 1414.2041 |
| 0.9 | 12 | 0.9 | 560196 | 46800 | 1414.2041 | 1414.2041 | 1414.2041 |
| 0.9 | 1 | 3 | 560196 | 46800 | 1410.4076 | 1410.4076 | 1410.4076 |
| 0.9 | 3 | 3 | 164736 | 46800 | 1410.4076 | 1410.4076 | 1410.4076 |
| 0.9 | 6 | 3 | Error in Fluent - Diverge | | | | |
| 0.9 | 9 | 3 | 165438 | 46800 | Error in Fluent | | |
| 1.8 | 3 | 3 | 162162 | 46800 | 1386.5411 | 1386.5411 | 1386.5411 |
| 0.9 | 12 | 3 | 167544 | 46800 | 1414.2041 | 1414.2041 | 1414.2041 |
| 0.9 | 3 | 4.5 | Error in Meshing | | | | |
| 0.9 | 1 | 6 | 560196 | 46800 | 1410.4076 | 1410.4076 | 1410.4076 |
| 0.9 | 6 | 6 | Error in Meshing | | | | |
| 0.9 | 9 | 6 | Error in Meshing | | | | |
| 0.9 | 12 | 6 | Error in Meshing | | | | |
| 0.9 | 1 | 9 | 560196 | 46800 | 1410.4076 | 1410.4076 | 1410.4076 |
| 0.9 | 6 | 9 | Error in Meshing | | | | |
| 0.9 | 9 | 9 | Error in Meshing | | | | |
| 0.9 | 12 | 9 | Error in Meshing | | | | |
| 0.9 | 1 | 90 | 560196 | 46800 | 1410.4076 | 1410.4076 | 1410.4076 |

Table 4.2: Size function variable for blade (with same Size Limit for comparison)

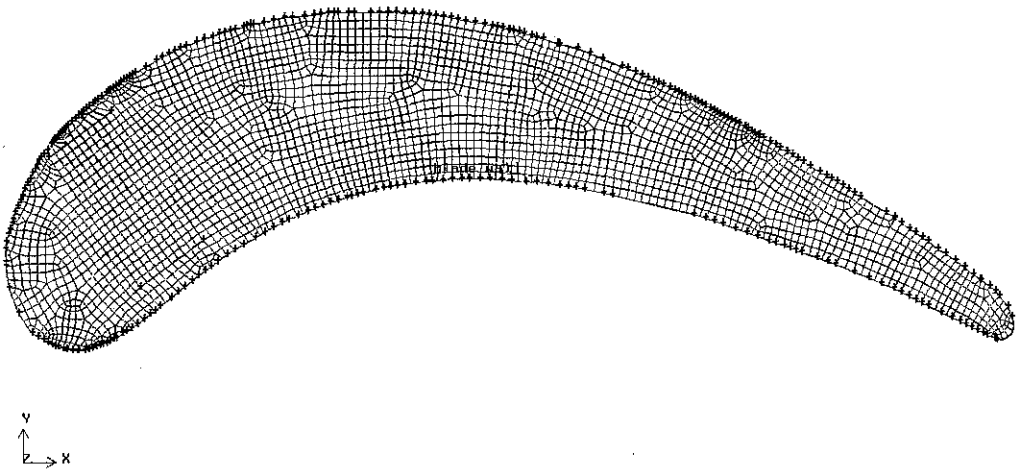


Figure 4.2: Blade Size Function 0.9-1-0.9

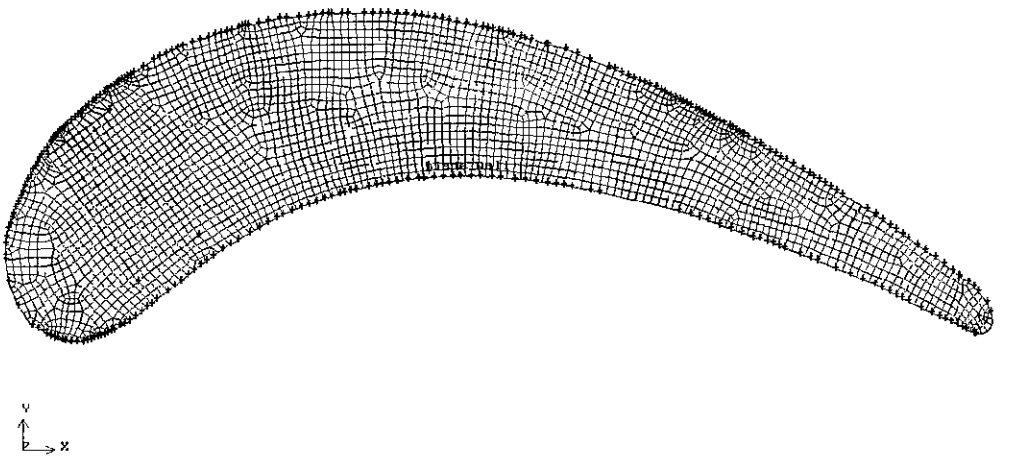


Figure 4.3: Blade Size Function 0.9-3-0.9

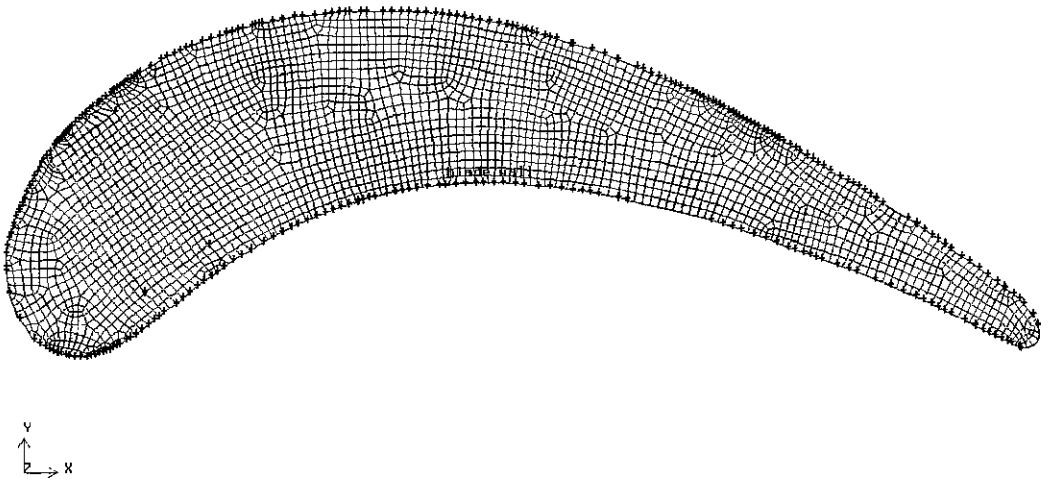

Figure 4.4: Blade Size Function 0.9-9-0.9

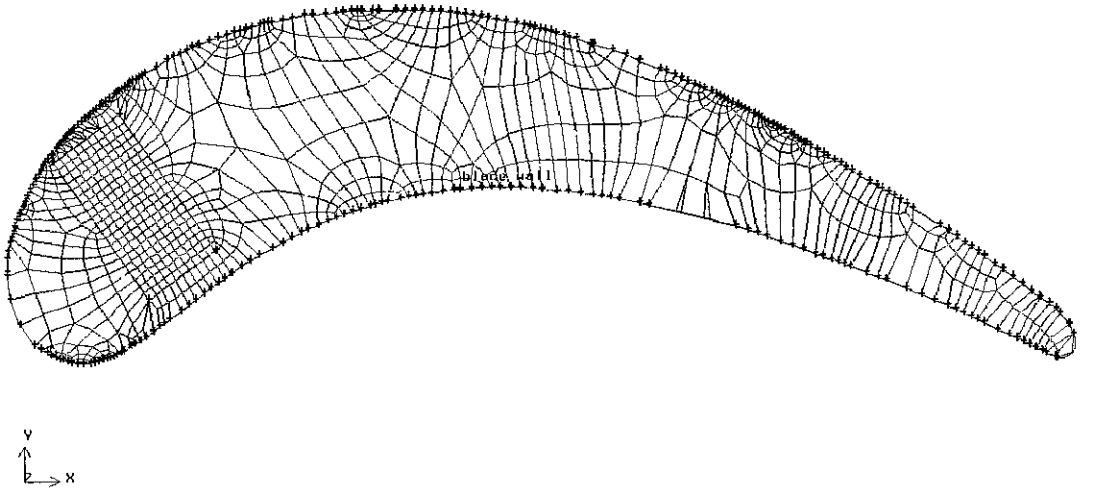

Figure 4.5: Blade Size Function 0.9-3-3

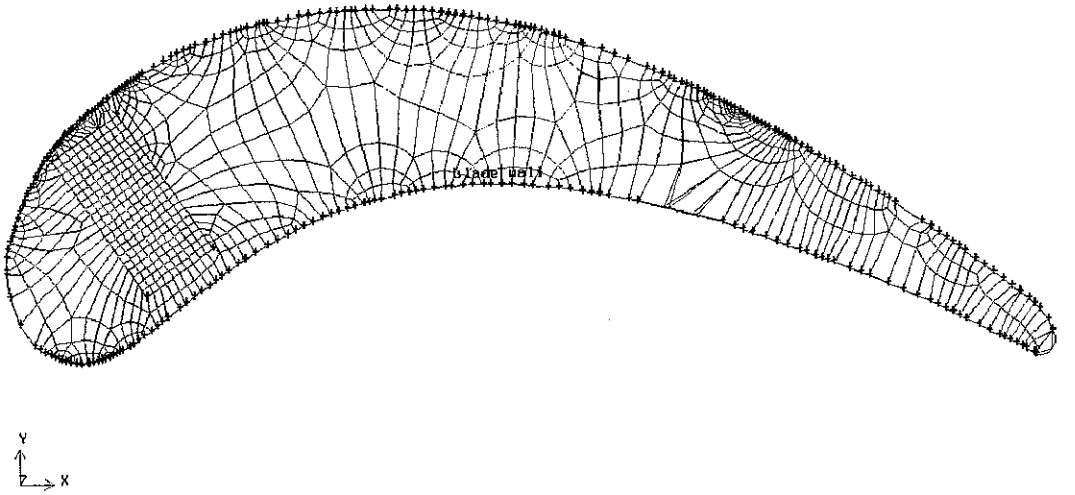

Figure 4.6: Blade Size Function 0.9-9-3

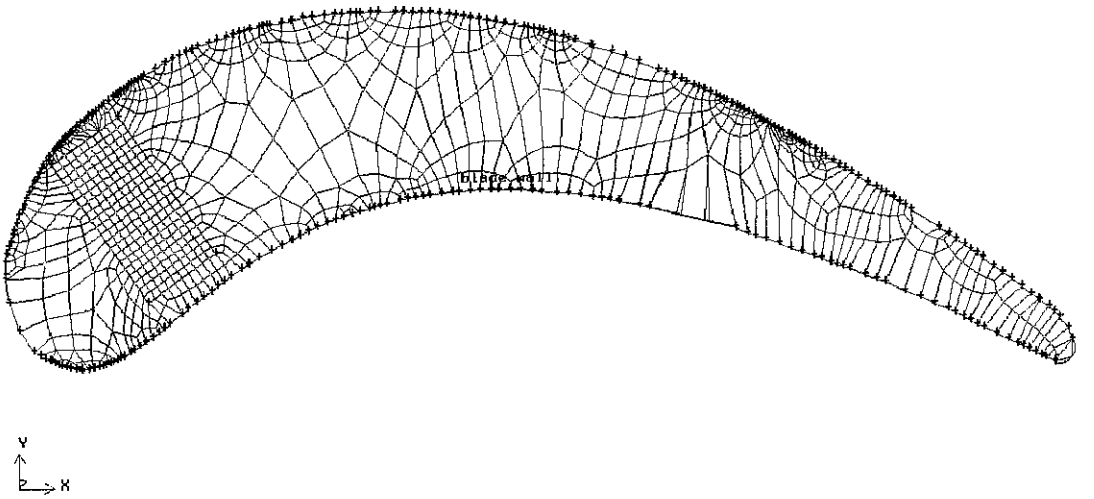

Figure 4.7: Blade Size Function 0.9-12-3

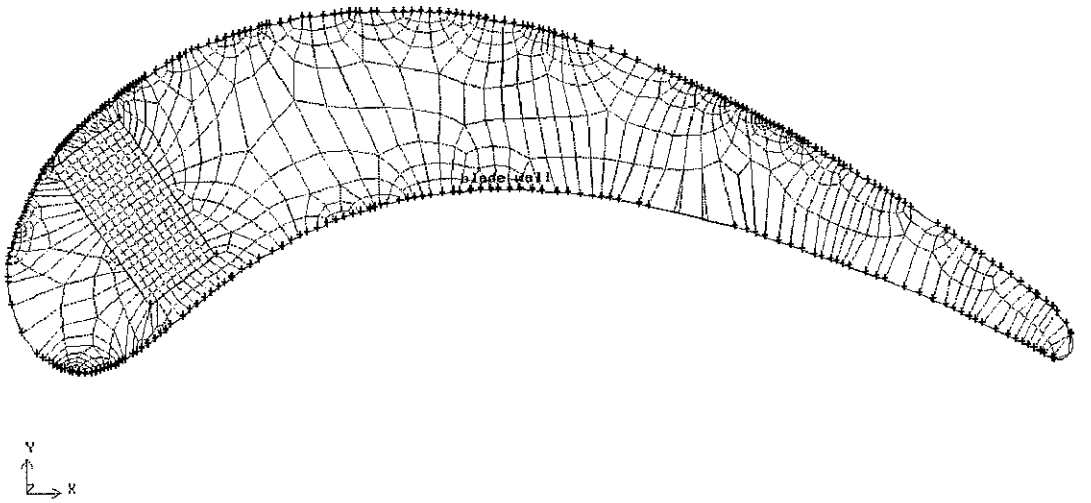


Figure 4.8: Blade Size Function 1.8-3-3

The criteria to choose the size function for blade are two;

- the temperature (if it does not have error in meshing) &
- the total element

From Table 4.1 & Table 4.2, we can see that even though the size limit is changing for a constant growth rate of 1, the temperature does not affect the meshed blade. Thus we increase the growth rate to 3, 6, 9 & 12 for different size limit of 0.9, 3, 6, 9, & 90.
The selected size function with starting size of 0.9 is 0.9-3-3. This is because it has less total element so that it reduce the load of the software while running in Fluent later on. Starting size of 0.9 and 1.8 also used to compare after size function with starting size of 0.9 has been chosen (0.9-3-3). Size function (1.8-3-3) has a lower number of total element, 162162, compare to size function (0.9-3-3) which has 164736 elements. Size function of 0.9-3-3 and 1.8-3-3 will be used to determine channel size function.

### 4.1.2 CHANNEL SIZE FUNCTION

| Size Function | | | Blade Size Function | Meshing (in Gambit) |
|---|---|---|---|---|
| Start Size | Growth Rate | Size Limit | | |
| 0.9 | 1 | 0.9 | 0.9-3-3 | ✓ |
| 0.9 | 1 | 1.8 | 1.8-3-3 | ✓ |
| 0.9 | 1 | 0.9 | 0.9-3-3 | ✓ |
| 0.9 | 1 | 1.8 | 1.8-3-3 | ✓ |
| 0.9 | 2 | 0.9 | 0.9-3-3 | ✓ |
| 0.9 | 2 | 1.8 | 1.8-3-3 | ✓ |
| 0.9 | 2 | 0.9 | 0.9-3-3 | ✓ |
| 0.9 | 2 | 1.8 | 1.8-3-3 | Error |
| 0.9 | 3 | 0.9 | 0.9-3-3 | ✓ |
| 0.9 | 3 | 1.8 | 1.8-3-3 | ✓ |
| 0.9 | 3 | 0.9 | 0.9-3-3 | ✓ |
| 0.9 | 3 | 1.8 | 1.8-3-3 | ✓ |
| 1.8 | 1 | 0.9 | 0.9-3-3 | Error |
| 1.8 | 1 | 1.8 | 1.8-3-3 | Error |
| 1.8 | 1 | 0.9 | 0.9-3-3 | ✓ |
| 1.8 | 1 | 1.8 | 1.8-3-3 | Error |
| 1.8 | 2 | 0.9 | 0.9-3-3 | Error |
| 1.8 | 2 | 1.8 | 1.8-3-3 | Error |
| 1.8 | 2 | 0.9 | 0.9-3-3 | ✓ |
| 1.8 | 2 | 1.8 | 1.8-3-3 | Error |
| 1.8 | 3 | 0.9 | 0.9-3-3 | Error |
| 1.8 | 3 | 1.8 | 1.8-3-3 | Error |
| 1.8 | 3 | 0.9 | 0.9-3-3 | ✓ |
| 1.8 | 3 | 1.8 | 1.8-3-3 | Error |

Table 4.3: Channel size function configuration meshing

Some errors occur in certain size function. One of the reasons is because from the channel size limit 1.8, it cannot be started with size 0.9 at the channel (Refer Figure 4.9). Thus, different growth rate can eliminate those errors.

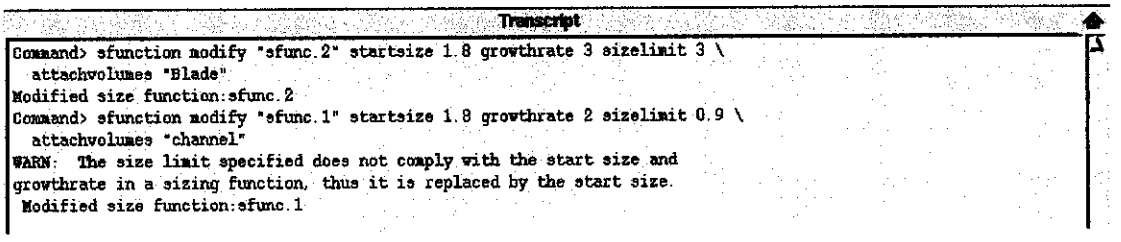


Figure 4.9: Size Function Error

| Size Function | | | Blade Size Function | Total Element | | Temperature (Kelvin) | | |
|---|---|---|---|---|---|---|---|---|
| Start Size | Growth Rate | Size Limit | | Channel | Blade | Point A | Point B | Point C |
| 0.9 | 1 | 0.9 | 0.9-3-3 | 46800 | 164736 | 1237.7634 | 1383.265 | 1383.265 |
| 0.9 | 1 | 0.9 | 1.8-3-3 | 46800 | 162162 | 1468.8895 | 1386.6672 | 1386.6672 |
| 0.9 | 1 | 1.8 | 0.9-3-3 | 46800 | 164736 | 1382.6672 | 1382.6672 | 1382.6672 |
| 0.9 | 1 | 1.8 | 1.8-3-3 | 46800 | 162162 | 1468.3405 | 1386.1664 | 1386.1664 |
| 0.9 | 2 | 0.9 | 0.9-3-3 | 46800 | 166374 | 1390.2856 | 1390.2856 | 1390.2856 |
| 0.9 | 2 | 0.9 | 1.8-3-3 | 46800 | 162162 | 1468.7209 | 1386.5117 | 1386.5117 |
| 0.9 | 2 | 1.8 | 0.9-3-3 | 33507 | 155052 | 1413.9799 | 1413.9799 | 1413.9799 |
| 0.9 | 3 | 0.9 | 0.9-3-3 | 46800 | 164736 | 1383.265 | 1383.265 | 1383.265 |
| 0.9 | 3 | 0.9 | 1.8-3-3 | 46800 | 162162 | 1468.7209 | 1386.5117 | 1386.5117 |
| 0.9 | 3 | 1.8 | 0.9-3-3 | 33507 | 155052 | 1398.1931 | 1398.1931 | 1398.1931 |
| 0.9 | 3 | 1.8 | 1.8-3-3 | 10530 | 78507 | 1359.7894 | 1359.7894 | 1359.7894 |
| 1.8 | 1 | 1.8 | 0.9-3-3 | 29784 | 147606 | 1362.3967 | 1362.3967 | 1362.3967 |
| 1.8 | 2 | 1.8 | 0.9-3-3 | 29784 | 147606 | 1362.3967 | 1362.3967 | 1362.3967 |
| 1.8 | 3 | 1.8 | 0.9-3-3 | 29784 | 147606 | 1362.3967 | 1362.3967 | 1362.3967 |

Table 4.4 Size function variable for channel

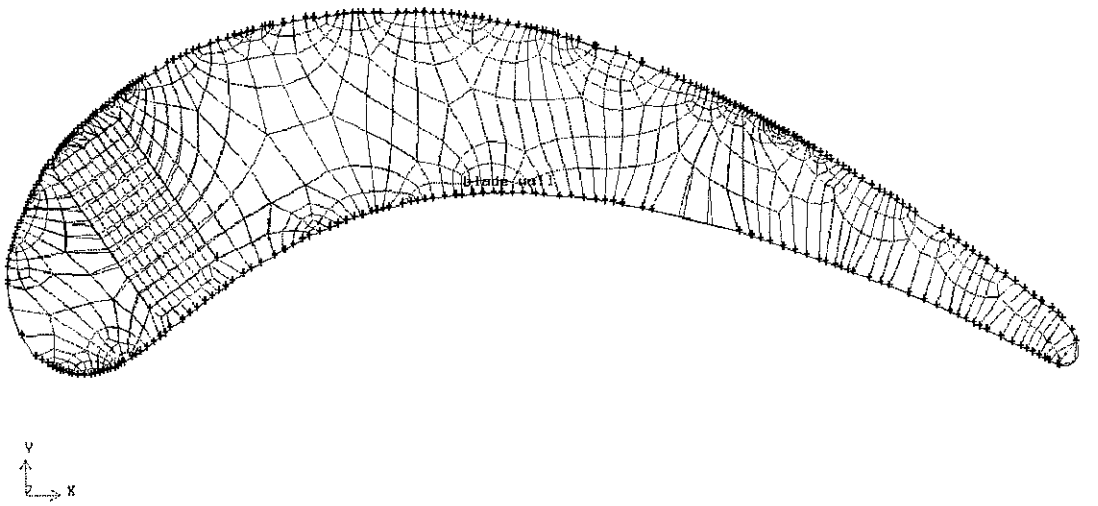

Figure 4.10: Channel Size Function 0.9-3-1.8 (1.8-3-3)

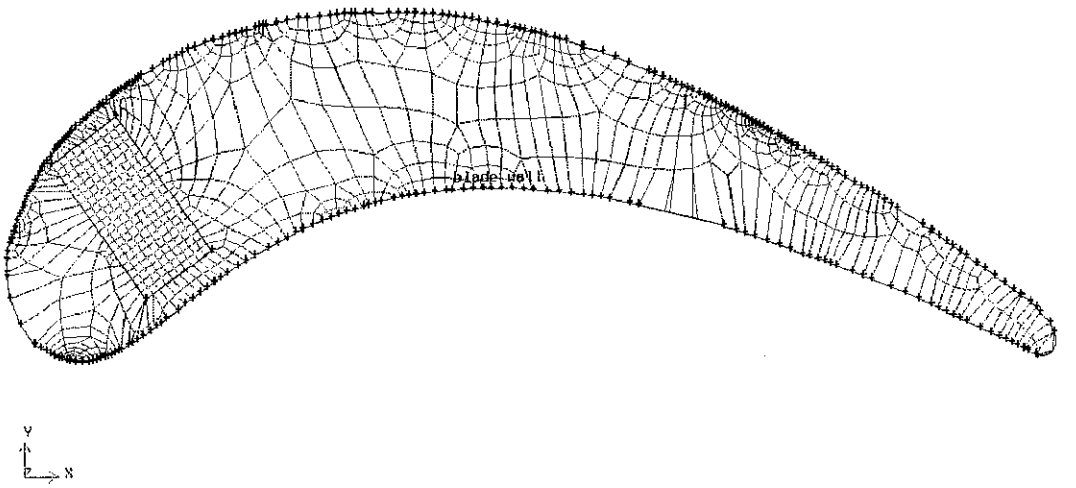

Figure 4.11 Channel Size Function 0.9-1-1.8 (1.8-3-3)

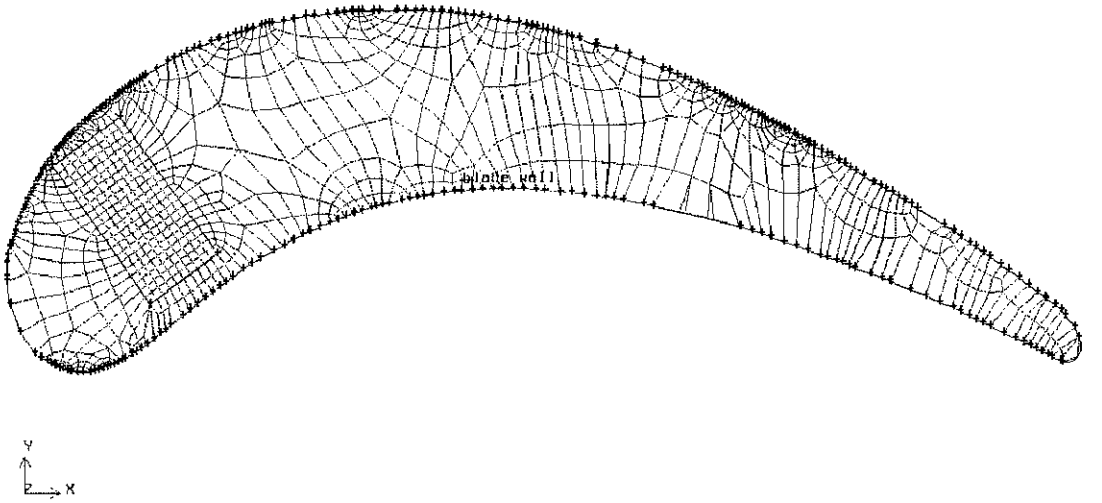


Figure 4.12: Channel Size Function 0.9-3-0.9 (0.9-3-3)

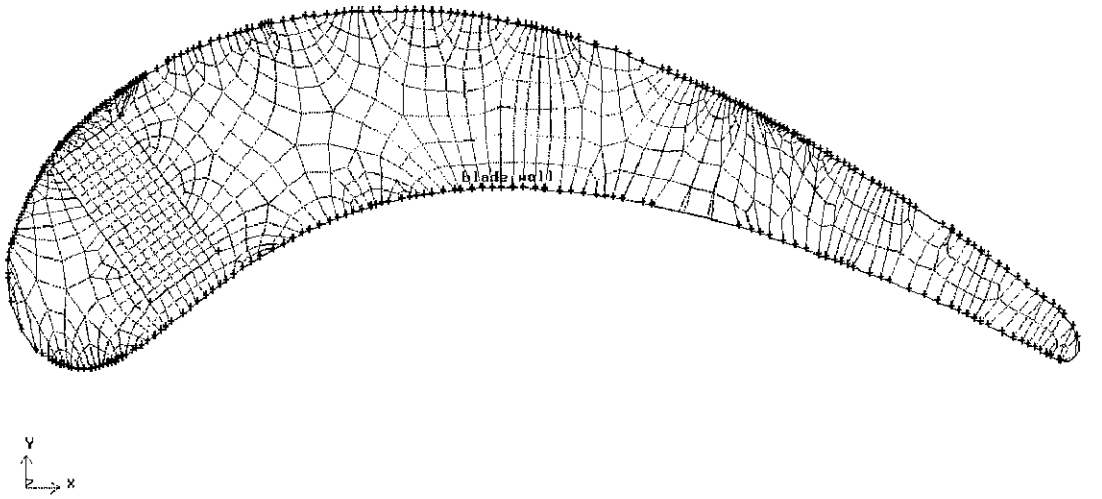


Figure 4.13 Channel Size Function 1.8-1-1.8 (0.9-3-3)

From Table 4.4, Point A, B & C has reached the lowest temperature difference among the configuration which is 50.62K or 3.5% comparing 1359.7894K with 1410.4076K. This temperature different has not exceed the limit that we have set that is 5% temperature different. Thus channel size function 0.9-3-1.8 and blade size function 1.8-3-3 has been chosen and use for the simulation.

## 4.2 SMOOTH CHANNEL

After the size function is determined using grid independency, the blade which is in Gambit (Figure 4.14) will be exported to Fluent for simulation purposes.

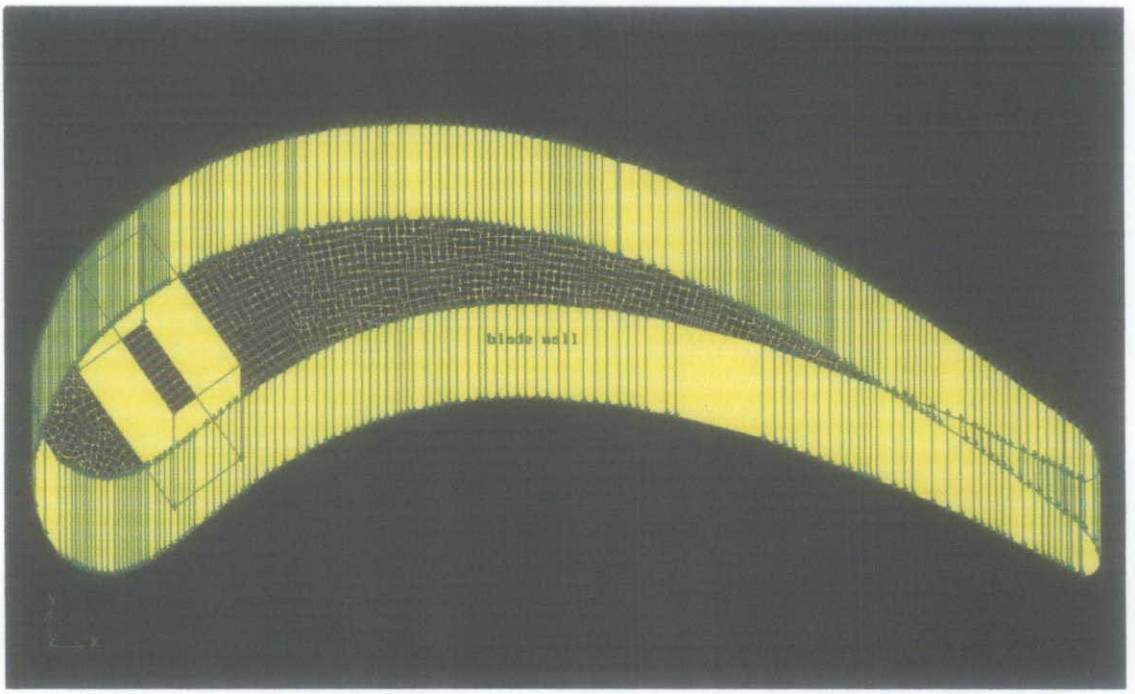


Figure 4.14: Blade in Gambit to be exported to Fluent

Once the setting and boundary condition have been set in Fluent, the result will be showed as figure below:

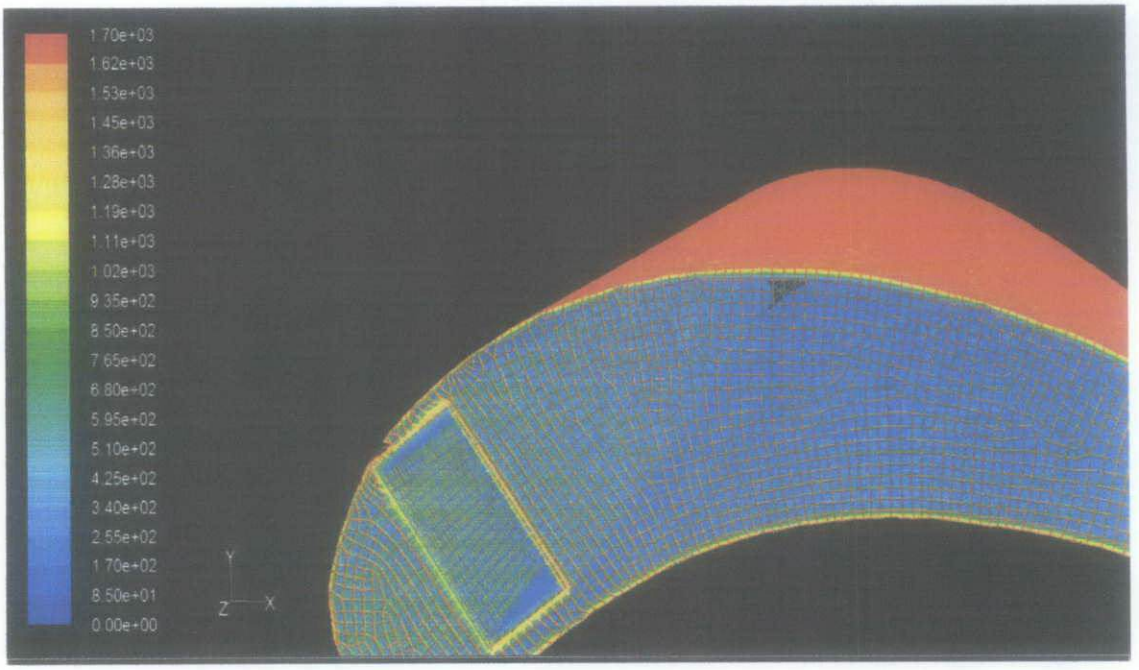


Figure 4.15 Fluent Simulation Result

The temperature on the smooth channel blade will be compared to the result which is done using analytical method (Matlab). The X-Axis and Y-axis has to be determined so that it will be easier to be compare in a specific direction.

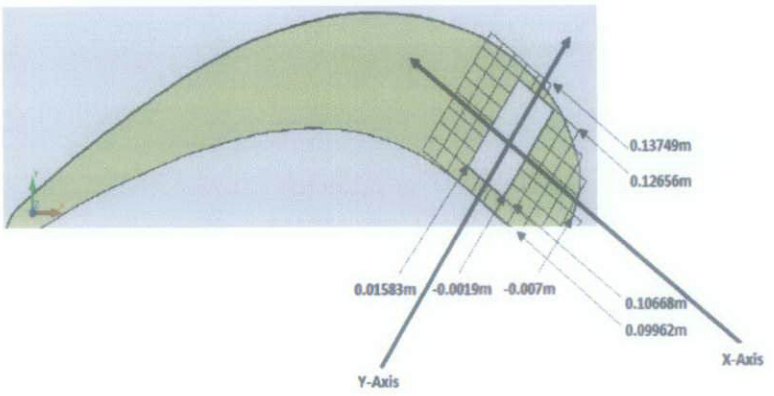


Figure 4.16: Temperature direction in X-Axis & Y-Axis

| | | | | | | | | | | | |
|---|---|---|---|---|---|---|---|---|---|---|---|
| T1 | T2 | T3 | T4 | T5 | T6 | | | | | | |
| 1519 | 1517 | 1514 | 1512 | 1522 | 1538 | | | | | | |
| T7 | T8 | T9 | T10 | T11 | T12 | T13 | T14 | T15 | | | |
| 1498 | 1496 | 1491 | 1484 | 1497 | 1515 | 1554 | 1577 | 1595 | | | |
| T16 | T17 | T18 | T19 | | | T20 | T21 | T22 | T23 | | |
| 1482 | 1479 | 1470 | 1452 | | | 1541 | 1566 | 1587 | 1605 | | |
| T24 | T25 | T26 | T27 | | | T28 | T29 | T30 | T31 | T32 | |
| 1471 | 1468 | 1457 | 1437 | | | 1533 | 1559 | 1581 | 1600 | 1616 | |
| T33 | T34 | T35 | T36 | | | T37 | T38 | T39 | T40 | T41 | |
| 1467 | 1464 | 1452 | 1432 | | | 1530 | 1556 | 1578 | 1597 | 1612 | |
| T42 | T43 | T44 | T45 | | | T46 | T47 | T48 | T49 | T50 | T51 |
| 1471 | 1467 | 1457 | 1437 | | | 1530 | 1556 | 1578 | 1598 | 1616 | 1633 |
| T52 | T53 | T54 | T55 | | | T56 | T57 | T58 | T59 | T60 | T61 |
| 1482 | 1479 | 1470 | 1452 | | | 1533 | 1559 | 1582 | 1601 | 1618 | 1633 |
| T62 | T63 | T64 | T65 | | | T68 | T69 | T70 | T71 | T72 | |
| 1498 | 1496 | 1491 | 1483 | 1496 | 1513 | 1540 | 1567 | 1588 | 1606 | 1621 | |
| T73 | T74 | T75 | T76 | T77 | T78 | T79 | T80 | T81 | T82 | | |
| 1518 | 1517 | 1514 | 1512 | 1521 | 1536 | 1557 | 1579 | 1598 | 1612 | | |

Smooth Channel

Figure 4.17: Temperature distribution at H=157.5mm to H=210mm [1]

The blade which is 210mm height (H or Z) is now divided into four sections which are 0-52.5mm. 52.5-105mm, 105-157.7mm, & 157.5-210mm. Figure 4.17 showing the temperature distribution at the bottom of the blade (H=157.5 mm to 210mm) done by previous study using analytical method. These readings are now compared to the temperature distribution in Figure 4.22 (for x-axis) & Figure 4.28 (for y-axis).

| | | | | | | | | | | | |
|---|---|---|---|---|---|---|---|---|---|---|---|
| T1 | T2 | T3 | T4 | T5 | T6 | | | | | | |
| 1502 | 1501 | 1497 | 1495 | 1506 | 1524 | | | | | | |
| T7 | T8 | T9 | T10 | T11 | T12 | T13 | T14 | T15 | | | |
| 1480 | 1478 | 1472 | 1465 | | | 1541 | 1567 | 1586 | | | |
| T16 | T17 | T18 | T19 | | | T20 | T21 | T22 | T23 | | |
| 1462 | 1459 | 1449 | 1430 | | | 1527 | 1555 | 1577 | 1597 | | |
| T24 | T25 | T26 | T27 | | | T28 | T29 | T30 | T31 | T32 | |
| 1450 | 1447 | 1435 | 1413 | | | 1519 | 1547 | 1571 | 1592 | 1609 | |
| T33 | T34 | T35 | T36 | | | T37 | T38 | T39 | T40 | T41 | |
| 1446 | 1442 | 1430 | 1408 | | | 1515 | 1543 | 1568 | 1588 | 1604 | |
| T42 | T43 | T44 | T45 | | | T46 | T47 | T48 | T49 | T50 | T51 |
| 1450 | 1446 | 1435 | 1413 | | | 1515 | 1543 | 1568 | 1589 | 1609 | 1627 |
| T52 | T53 | T54 | T55 | | | T56 | T57 | T58 | T59 | T60 | T61 |
| 1462 | 1459 | 1449 | 1430 | | | 1519 | 1547 | 1572 | 1592 | 1611 | 1628 |
| T62 | T63 | T64 | T65 | T66 | T67 | T68 | T69 | T70 | T71 | T72 | |
| 1480 | 1478 | 1472 | 1464 | 1478 | 1497 | 1526 | 1555 | 1578 | 1598 | 1615 | |
| T73 | T74 | T75 | T76 | T77 | T78 | T79 | T80 | T81 | T82 | | |
| 1502 | 1501 | 1497 | 1495 | 1505 | 1522 | 1545 | 1569 | 1589 | 1605 | | |

Smooth Channel

Figure 4.18: Temperature distribution at root of the blade (H=0mm) [1]

Meanwhile, Figure 4.18 shows the temperature distribution at the root or inlet of the channel and is compare to Figure 4.19 (for x-axis) & Figure 4.25 (for y-axis)..

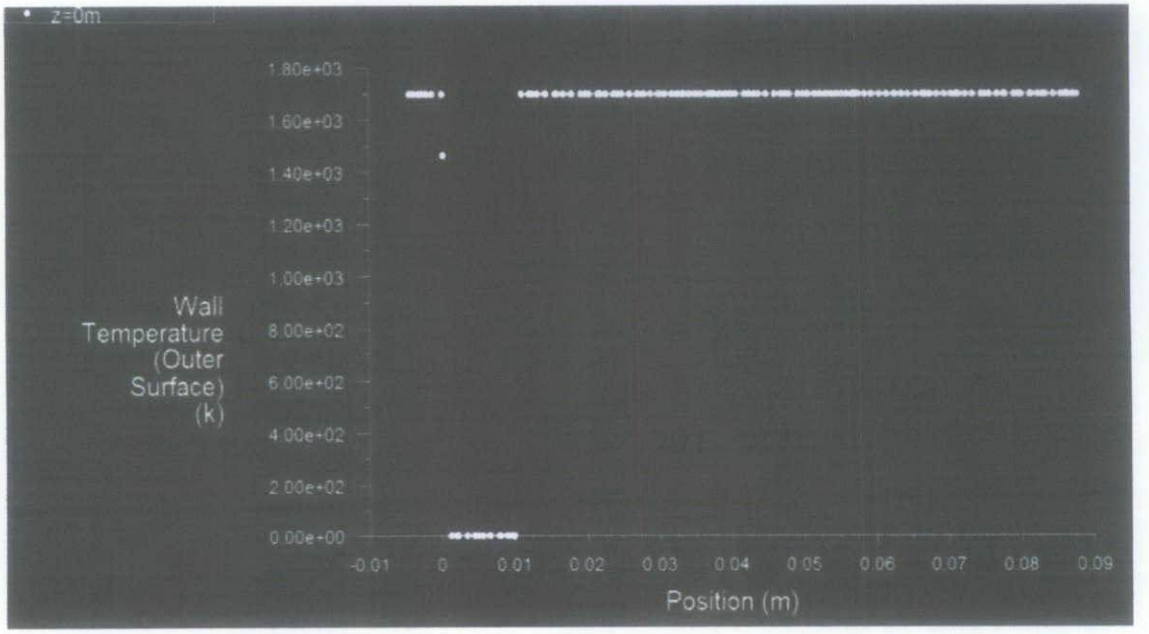


Figure 4.19: Temperature Distribution at (H=0mm) in X-axis

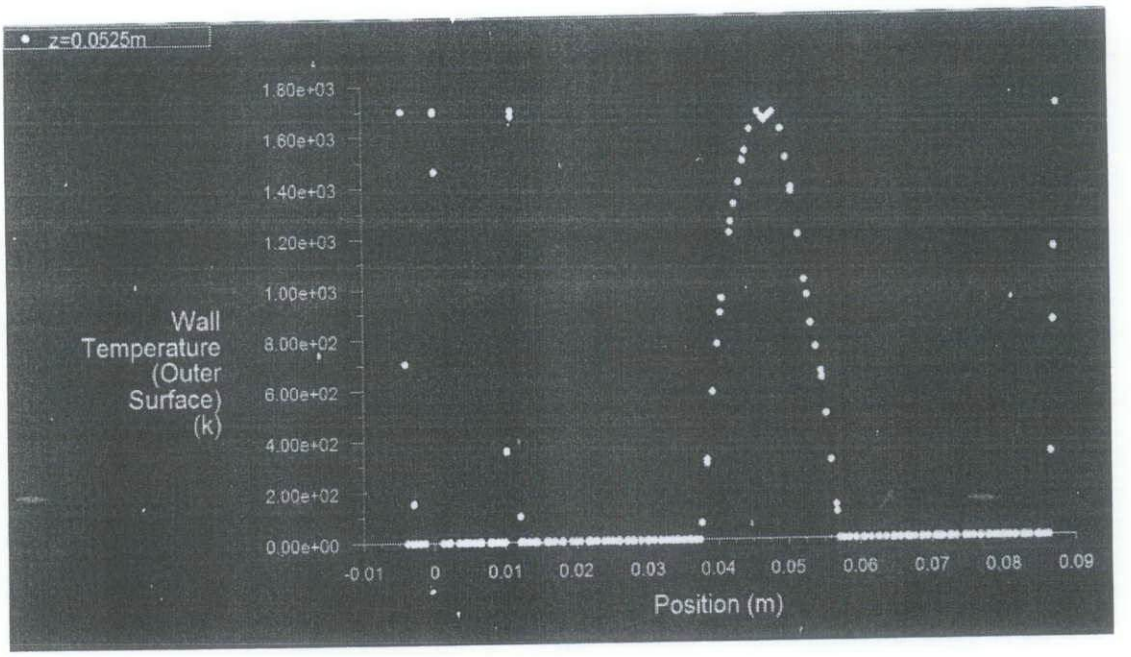


Figure 4.20: Temperature Distribution at (H=52.5mm) in X-axis

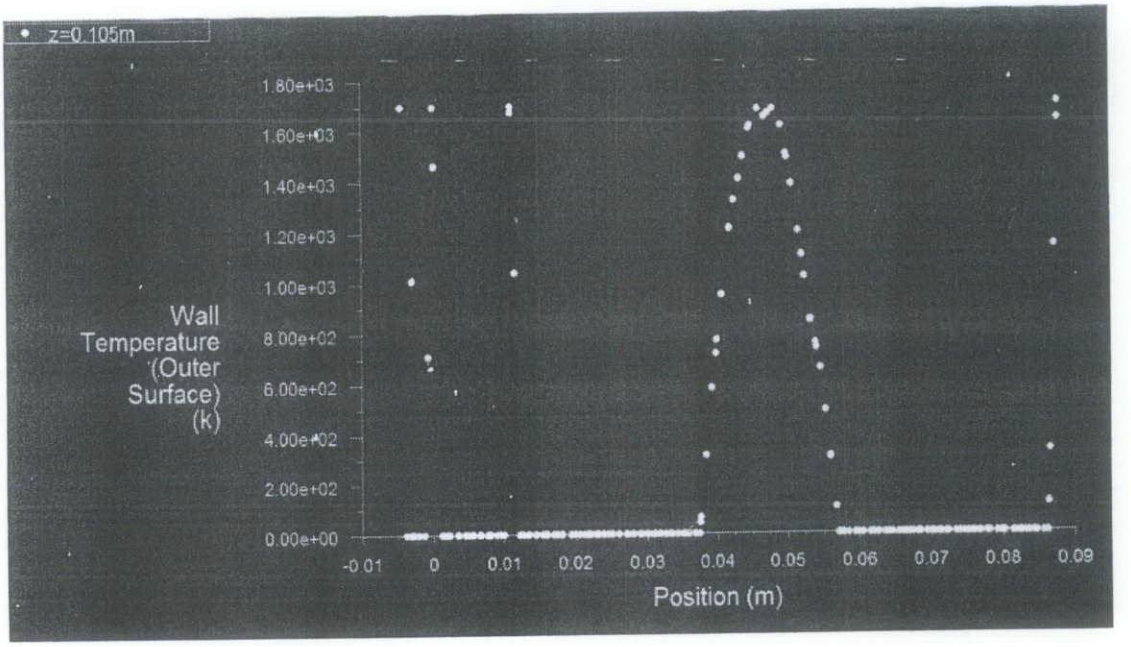


Figure 4.21: Temperature Distribution at (H=105mm) in X-axis

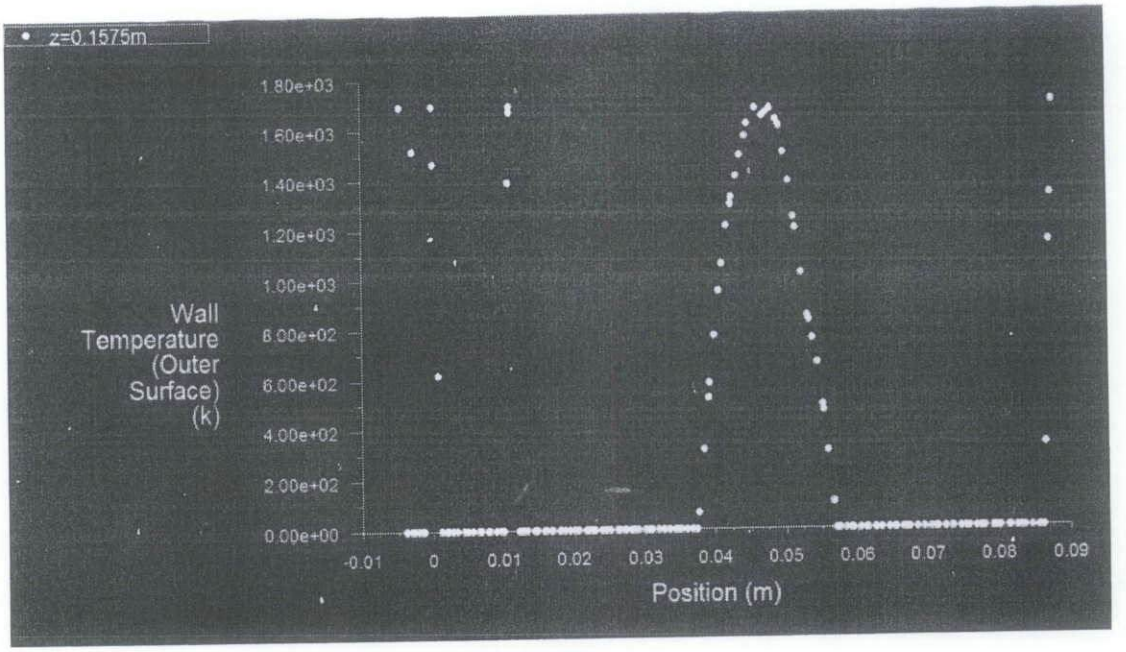


Figure 4.22: Temperature Distribution at (H=157.5mm) in X-axis

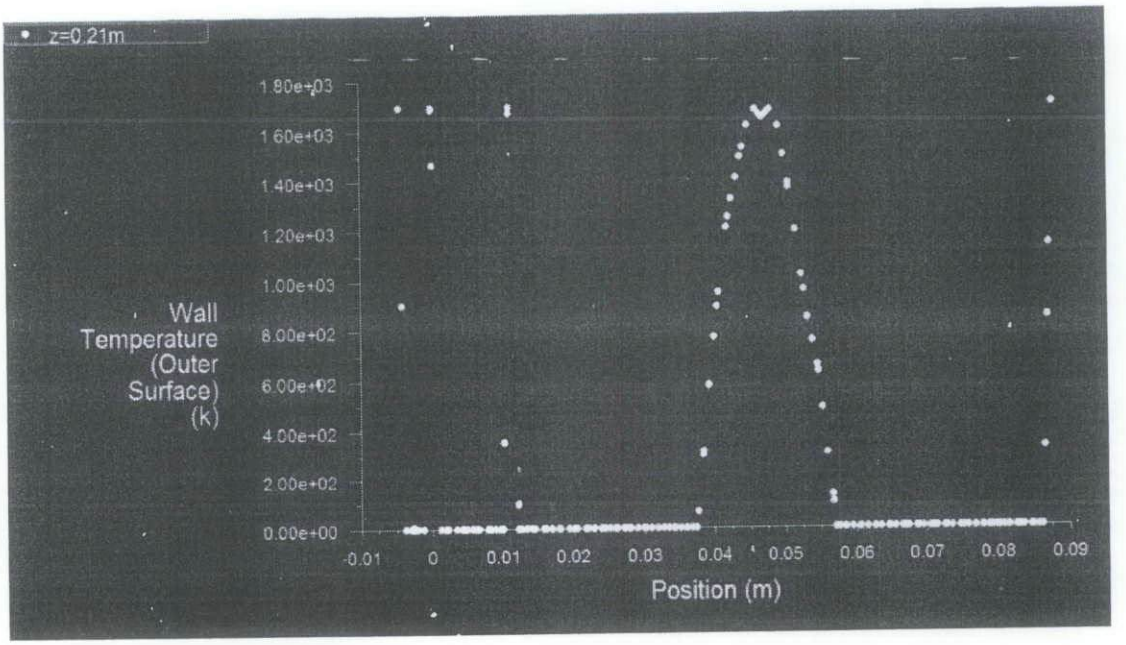


Figure 4.23: Temperature Distribution at (H=210mm) in X-axis

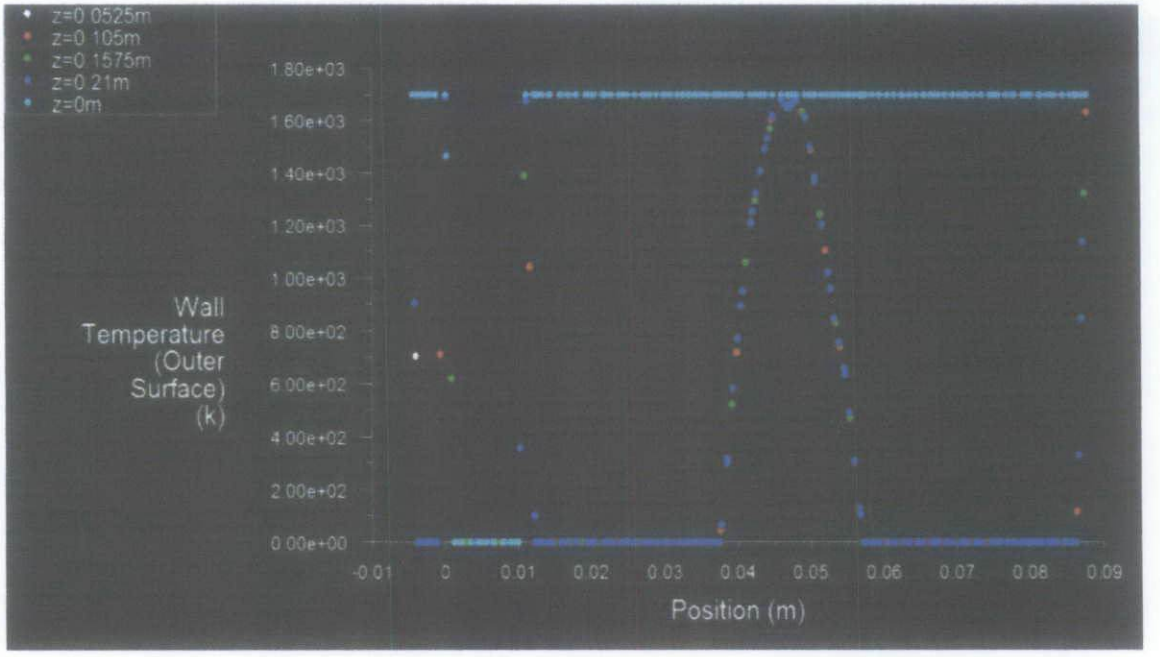


Figure 4.24: Temperature Distribution at (H=0mm to H=210mm) in X-axis

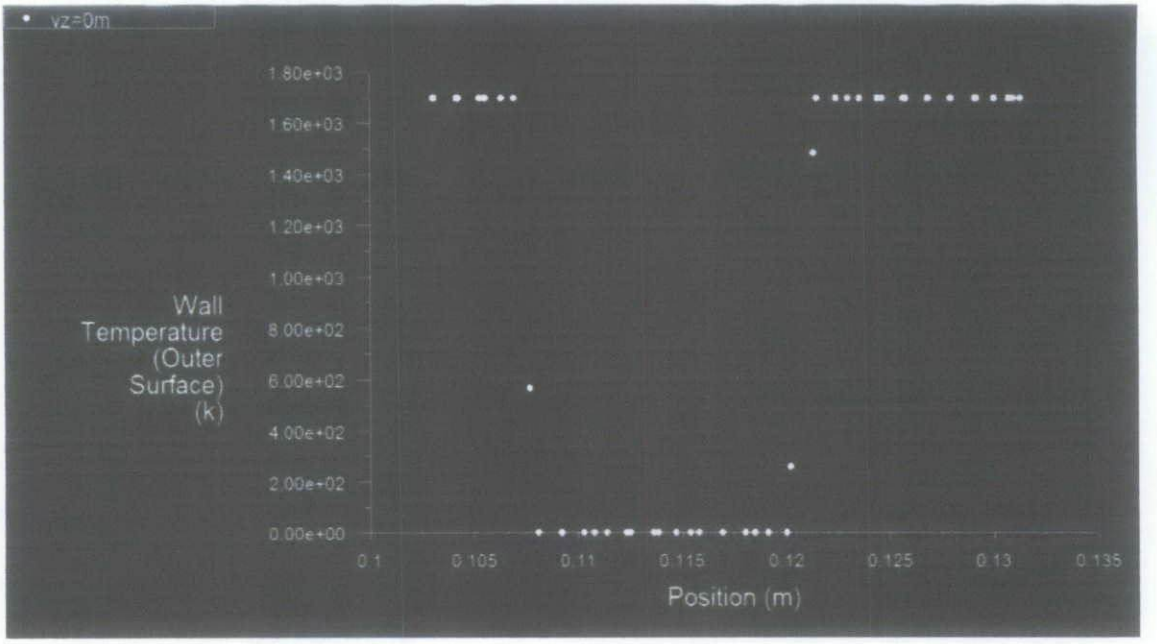


Figure 4.25: Temperature Distribution at (H=0mm) in Y-axis

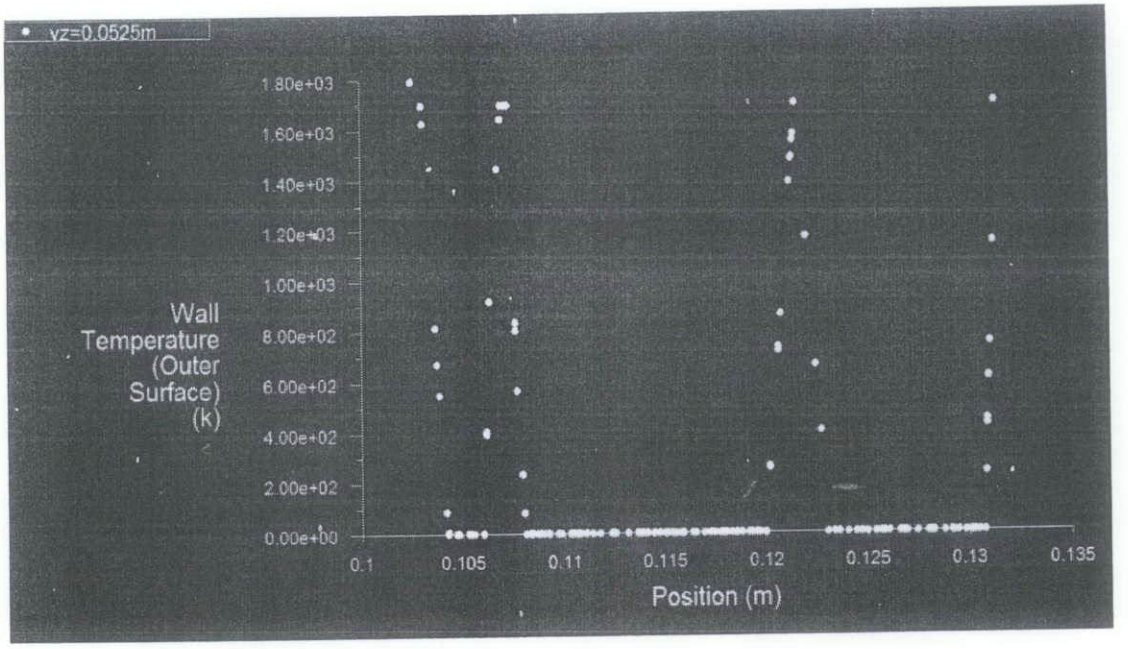


Figure 4.26: Temperature Distribution at (H=52.5mm) in Y-axis

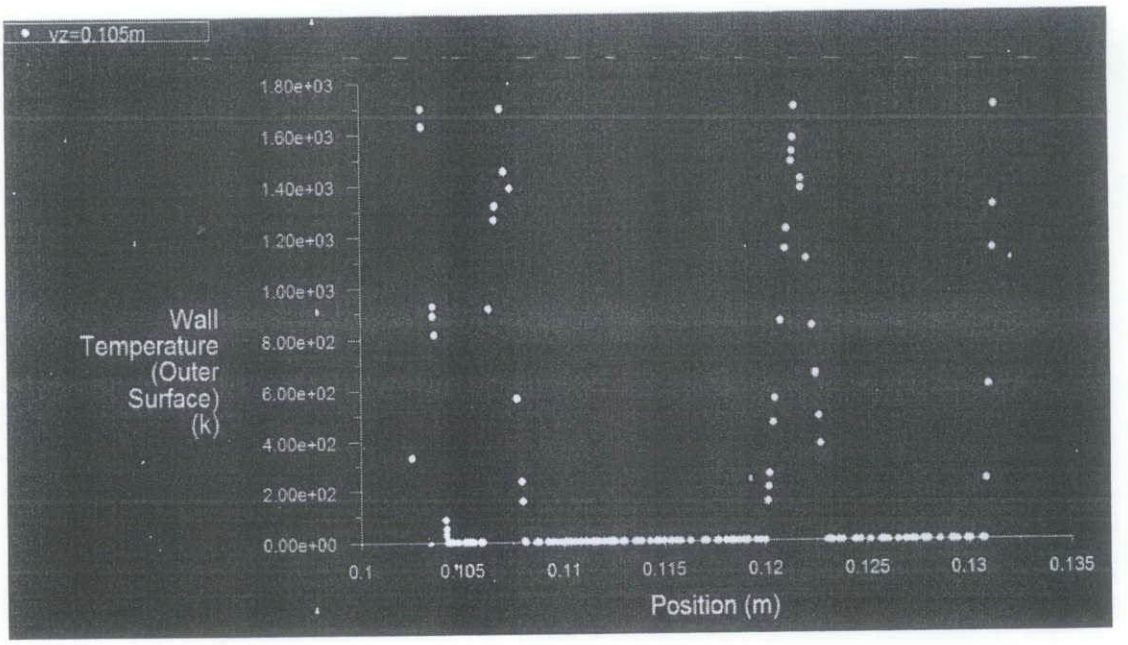


Figure 4.27: Temperature Distribution at (H=105mm) in Y-axis

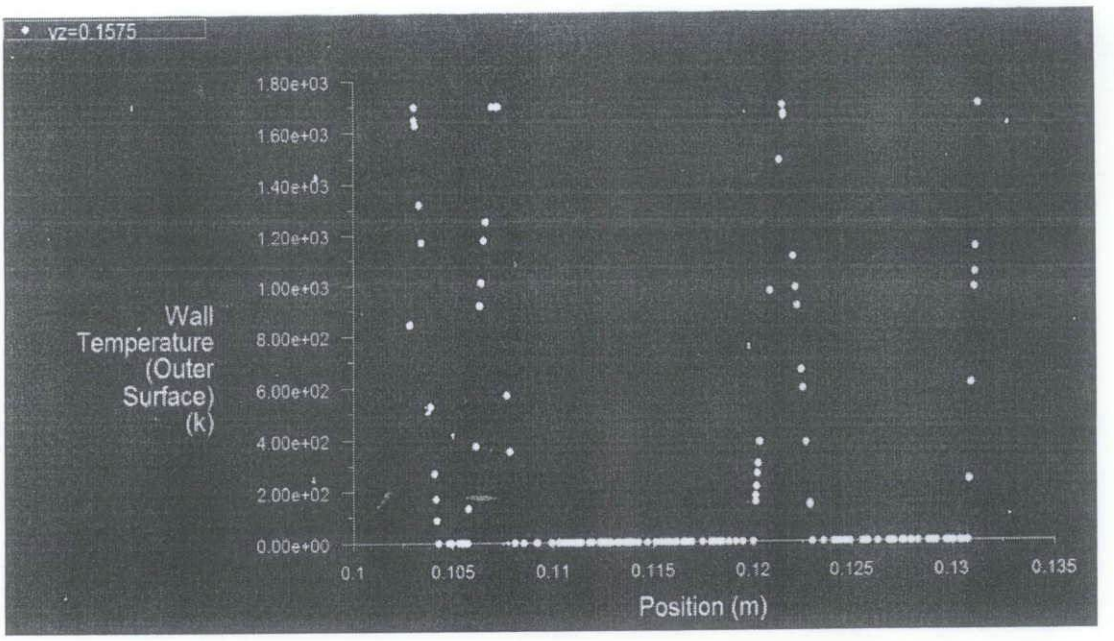


Figure 4.28: Temperature Distribution at (H=157.5mm) in Y-axis

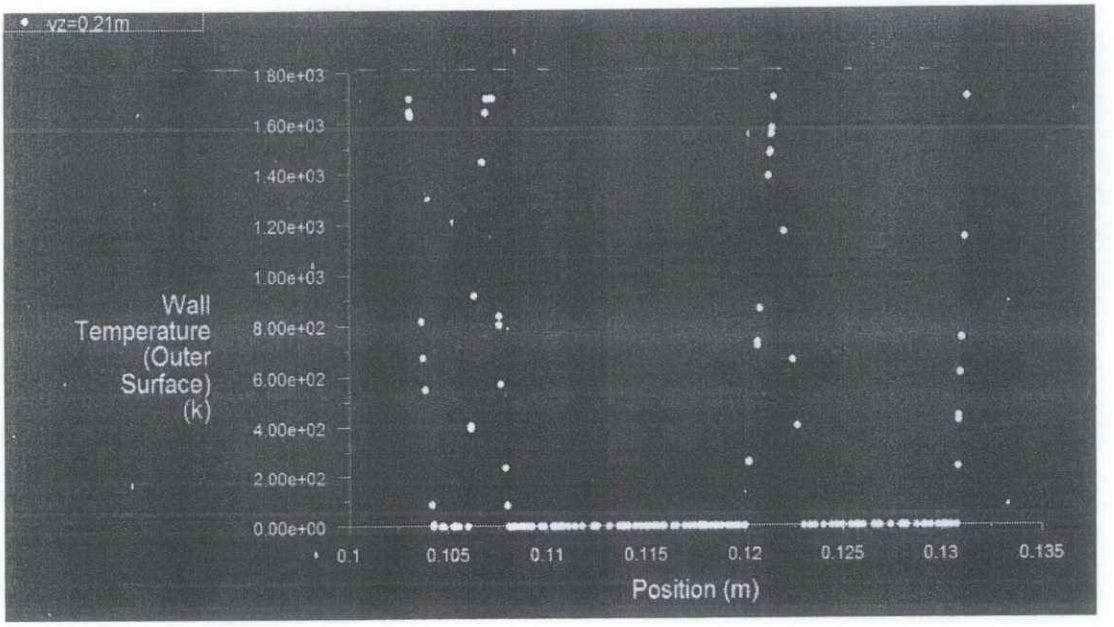


Figure 4.29: Temperature Distribution at (H=210mm) in Y-axis

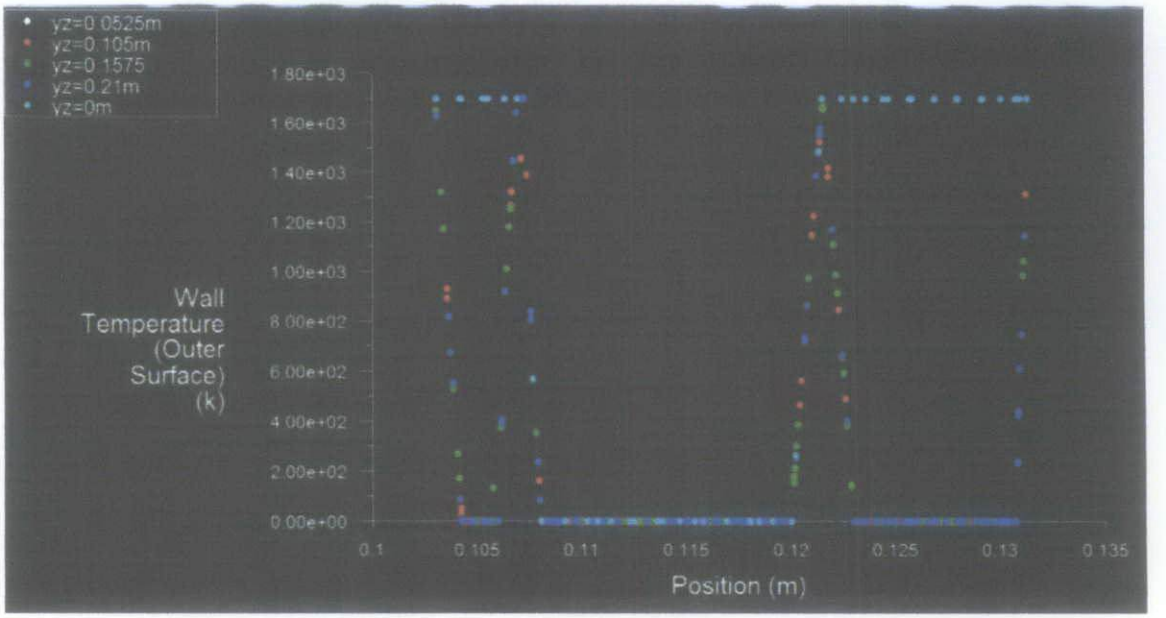


Figure 4.30: Temperature Distribution at (H=0 to H=210mm) in Y-axis

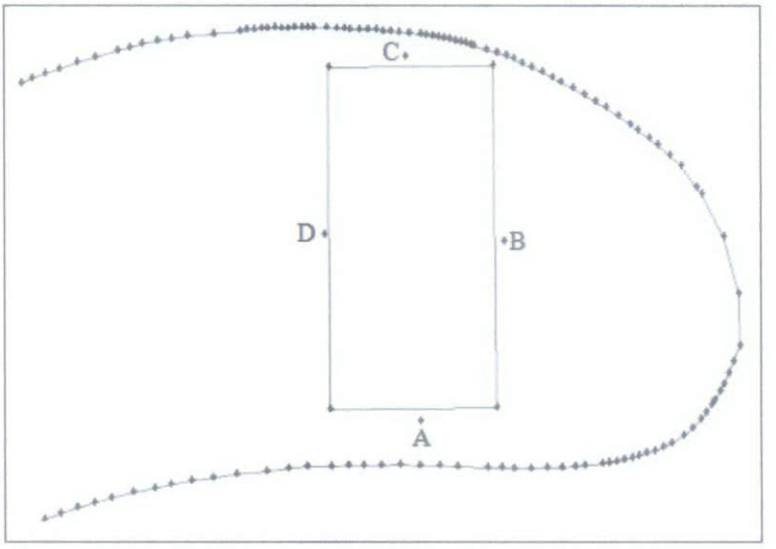


Figure 4.31: Temperature at 4 points near smooth channel

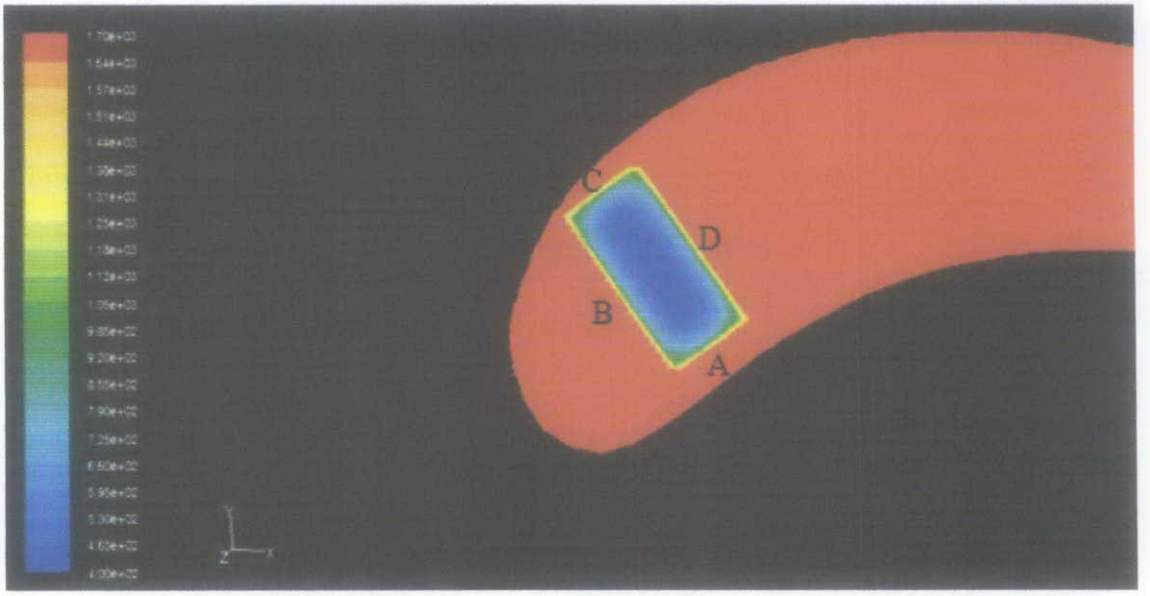


Figure 4.32: Temperature at 4 points near smooth channel showed in Fluent

In a more easy view, temperature at the four points showed in Figure 4.31 & Figure 4.33 will be compared to Figure 4.17 & Figure 4.18. The results are showed as below:

| Points | Temperature in Matlab (Kelvin) | | Temperature in Fluent (Kelvin) | Differences (%) |
|---|---|---|---|---|
| | Range/specific point | Average | | |
| A | 1496 - 1513 | 1504.5 | 1570.0005 | 4.35 |
| B | 1530 | 1530.0 | 1505.0005 | 1.64 |
| C | 1497 - 1515 | 1506.0 | 1505.0005 | 0.07 |
| D | 1432 | 1432.0 | 1440.0005 | 0.56 |

Table 4.5: Temperature differences between Matlab & Fluent at blade root

| Points | Temperature in Matlab (Kelvin) | | Temperature in Fluent (Kelvin) | Differences (%) |
|---|---|---|---|---|
| | Range/specific point | Average | | |
| A | 1478 – 1497 | 1487.5 | 1635.0006 | 9.92 |
| B | 1519 – 1515 | 1517.0 | 1635.0006 | 7.78 |
| C | 1506 – 1524 | 1515.0 | 1635.0006 | 7.92 |
| D | 1408 - 1413 | 1410.5 | 1635.0006 | 15.92 |

Table 4.6: Temperature differences between Matlab & Fluent at height, H-157.5mm

From the Table 4.5, we can see that the different using analytical method (Matlab) and using numerical method (ANSYS-FLUENT) has less than 5% temperature difference on the root of the blade. However, that depends on the height of the blade.

For the case in which we determine the temperature differences at the third section of the height of the channel (H=157.5mm) as shown in Table 4.6, the temperature differences are bigger especially at point D which is located toward the tail of the blade. We can see that the different is 15.92% at point D, while point A, B, & C having differences less than 10% comparing both method.

## 4.3 RIB CHANNEL

Studies have been done by previous student and found out that with including two opposite rib wall at the longest side of the rectangular channel, the maximum of convection coefficient can be achieved[1]. From Table 4.7 below, the convection coefficient for the ribbed channel is 559.32 W/m$^2$.K. Thus simulation is carried out for the ribbed channel for rib angle $\alpha = 60^{\circ}$, height-to-hydraulic-diameter ratio $e/D = 0.078$, & pitch-to-height ratio p/e = 8.

FRICTION FACTOR AND CONVECTION COEFFICIENT FOR RIBBED CHANNEL AT $\dot{m} = 0.01$ kg/s

| Rib Angle ($\alpha$) | R($e^+$) | $e/D$ | $\bar{f}$ | $H_{ribbed}$ (W/m$^2$.K) |
|---|---|---|---|---|
| 90 | 5 | 0.042 | 0.0144 | 377.71 |
| 90 | 5 | 0.047 | 0.0148 | 381.04 |
| 90 | 5 | 0.063 | 0.0162 | 388.53 |
| 90 | 5 | 0.078 | 0.0173 | 392.98 |
| 60 | 3.25 | 0.042 | 0.0179 | 512.48 |
| 60 | 3.25 | 0.047 | 0.0187 | 521.27 |
| 60 | 3.25 | 0.063 | 0.0212 | 543.53 |
| 60 | 3.25 | 0.078 | 0.0236 | 559.32 |
| 45 | 3.9 | 0.042 | 0.0163 | 482.91 |
| 45 | 3.9 | 0.047 | 0.0170 | 490.50 |
| 45 | 3.9 | 0.063 | 0.0189 | 509.25 |
| 45 | 3.9 | 0.078 | 0.0207 | 522.97 |
| 30 | 5.2 | 0.042 | 0.0141 | 433.96 |
| 30 | 5.2 | 0.047 | 0.0145 | 439.83 |
| 30 | 5.2 | 0.063 | 0.0158 | 453.73 |
| 30 | 5.2 | 0.078 | 0.0169 | 462.58 |

Table 4.7: Friction factor and convection coefficient for ribbed channel [1]

Rib Calculation

Channel length = 18mm = 0.018m

Channel width = 9mm = 0.009m

Channel height = 210mm = 0.21m

Hydraulic Diameter, D = 4A/P = [4*(0.018*0.009)]/[2*(0.018+0.009)] = 0.012m

For rib-blockage ratio e/D = 0.078, substitute D = 0.012m into the equation,

We get e = 0.936mm

For P/e = 8 & considering the rib height and the rib length is equal, we can calculate the pitch or the distance between two ribs.

P/e = 8 > P/(0.936)=8 > P =7.488mm

The number of ribs can be calculated as below:

(210mm-10.392mm)/7.488mm = 26.65 ≈ 26

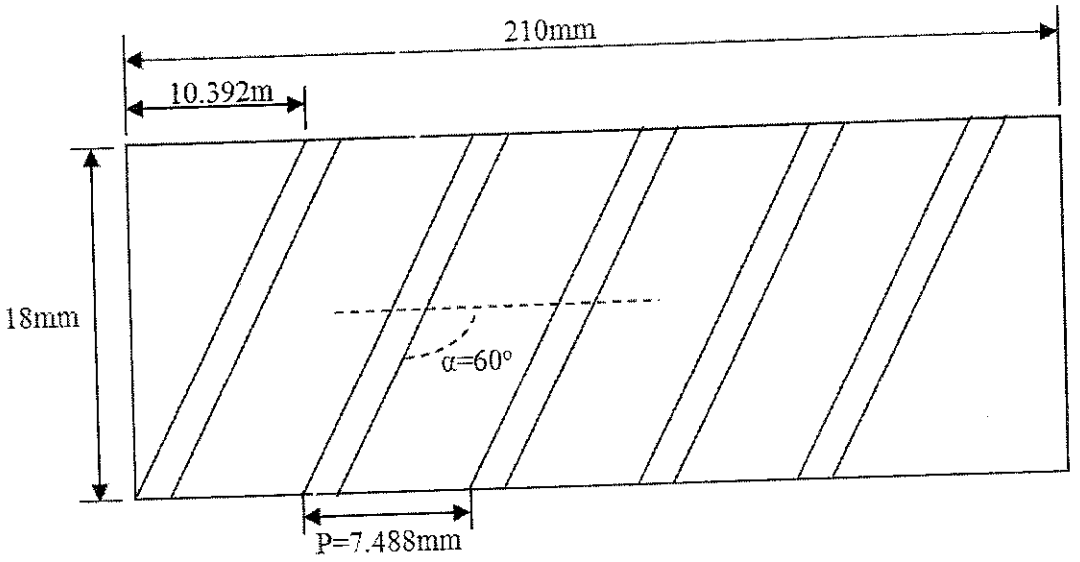


Figure 4.33 60° Rib Orientation

Figure 4.34 & 4.35 shows the temperature distribution of a smooth channel and a rib channel on Fluent

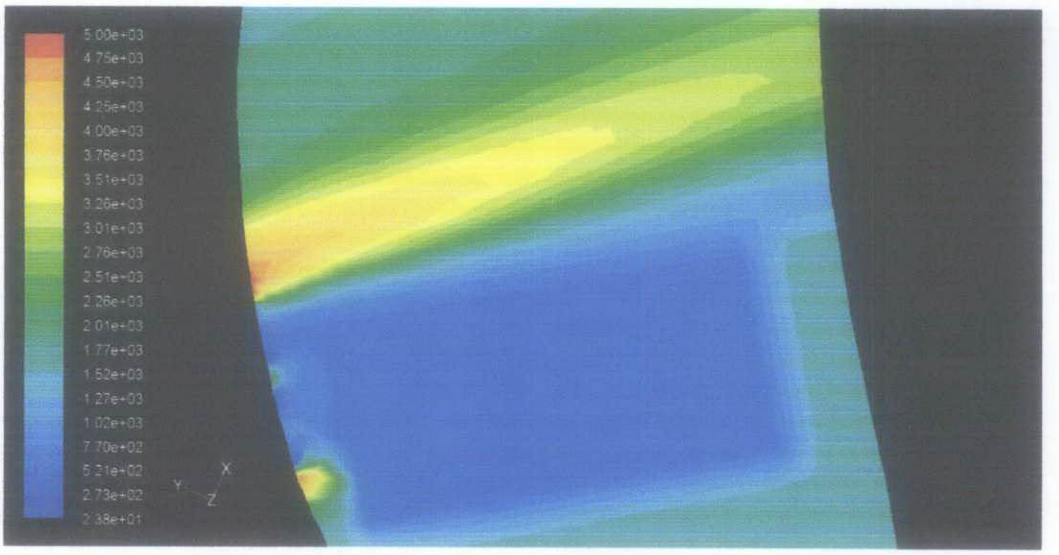


Figure 4.34: Temperature distribution of 60 degree rib

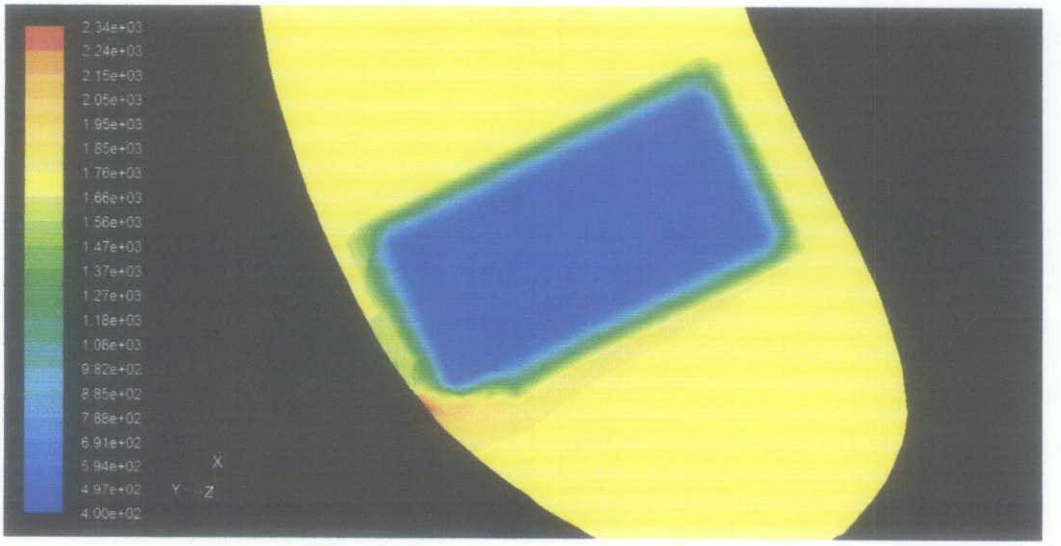


Figure 4.35: Temperature distribution of smooth channel

By looking at three points near the surface of the blade as in Figure 4.1, we can know the difference of having a two-opposite rib channel wall and a smooth channel wall.

| Channel Type | Temperature (Kelvin) | | |
|---|---|---|---|
| | Point A | Point B | Point C |
| Smooth | 1660.8119 | 1660.8119 | 1660.8119 |
| Rib | 1516.6266 | 1516.6266 | 1516.6266 |

Table 4.8 Temperature Differences between Smooth channel and Rib channel

$$\text{Rib Efficiency} = \frac{\text{(Smooth-Temperature – Rib-Temperature)}}{\text{Smooth-Temperature}} \times 100\%$$

$$= (1660.8119\text{K} - 1516.6266\text{K}) / 1660.8119\text{K} \times 100\%$$

$$= 8.68\%$$

# CHAPTER 5

# CONCLUSION AND RECOMMENDATION

## 5.1 CONCLUSION

The numerical analysis has been carried out using Gambit Modelling and Fluent simulation software. Gird independency is used to reduce the total number of elements in order to minimise the total time and load when running the simulation on Fluent. The best size function for the blade is starting size of 0.9, growth rate of 3, and size limit of 3. Using this size function 0.9-3-3 & 1.8-3-3 from the blade, the channel size function is now being determined. The lowest temperature difference among the configuration is 50.62K or 3.5%. This temperature different has not exceed the limit that we have set that is 5% temperature different. Thus channel size function 0.9-3-1.8 and blade size function 1.8-3-3 has been chosen and use for the simulation.

Comparison has been done on the smooth channel for analytical method (Matlab) and numerical method (ANSYS-FLUENT). The result is a satisfied result which is 4.35% or less than 5% temperature difference on the root of the blade. On the height of 157.5m, the temperature difference is slightly higher, mostly less than 10% except at point D which has 15.92%. This may due to the location which is located further behind and toward the tail of the blade.

A 60 degree rib angle with pitch-to-height ratio, p/e =8, and height-to-hydraulic-diameter, $e/D$=0.078 is carried out to compare the temperature difference with the smooth channel. The results shows with the specification of rib, we can cool the blade 8.68% more efficient.

## 5.2 RECOMMENDATION

Further detail analysis can be done by adding a far field around the blade. This is the hot gas compressed by the compressor and flow onto the blade. By adding far field, a more accurate data could be obtained. This added far field will cause the simulation to run/load harder as this far field volume would have a large number of elements. This means that it will add load to the computer to run the simulation.

With the current computer that the author is using, the Random Access Memory (RAM) is not sufficient to run the simulation. An upgraded RAM will definitely can run the blade together with the far field. Alternatively, more detail and advance in using Gambit should be focus so that the added far field can be simulated without upgrading computer's RAM.

Below is the example of added far field onto the blade in Gambit.

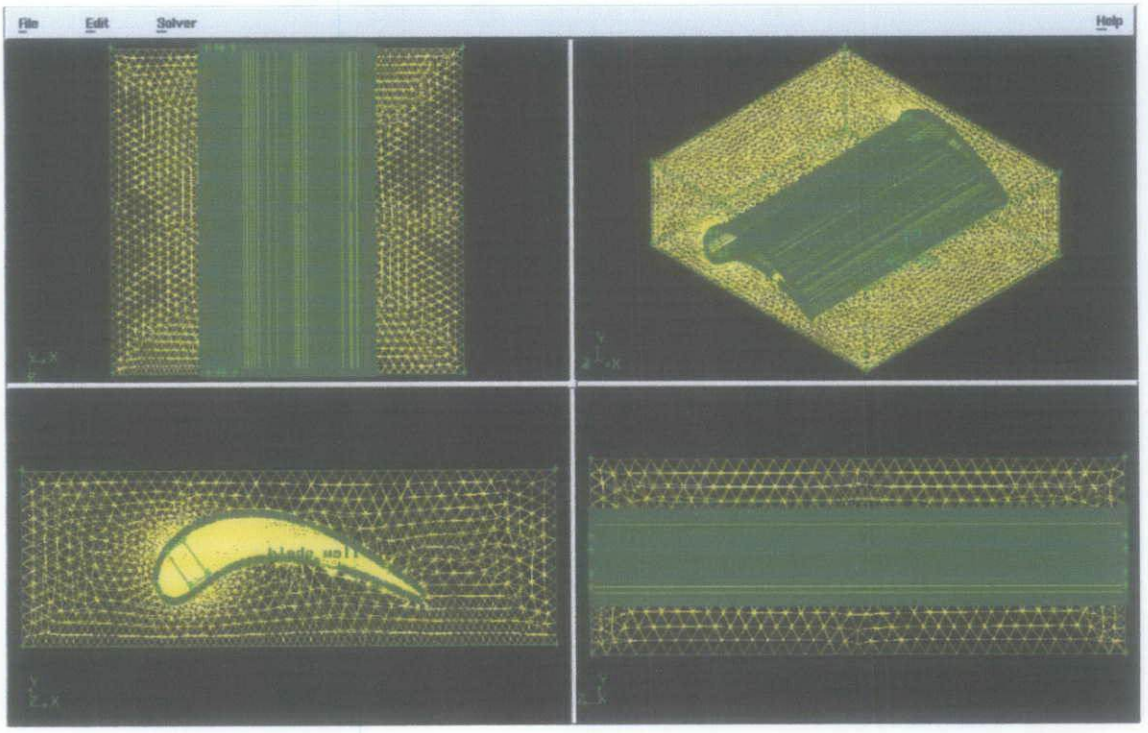


Figure 5.1: Gambit modelling with added far field

# REFERENCES


[1] Hussain h. Al-Kayeim and A. H. Ghanizadeh, 2010, *Analysis of the temperature Distribution in GT Blade Cooled by Compressed Air*, Universiti Teknologi PETRONAS, Malaysia.

[2] Je-Chin Han, Sandip Dutta and Srinath V. Ekkad, 2000, *Gas Turbine Heat Transfer and Cooling Technology*, Taylor & Francis.

[3] William Mc Donald, 2008, *Optimized Film Cooling Hole Design*, Internship Report, University of Central Florida.

[4] HIH Saravanamuttoo, GFC Rogers and H Cohen, 2001, *Gas Turbine Theory, 5th Edition*, Pearson Education Limited.

[5] Marc Johannes Noot, 1997, *Numerical Analysis of Turbine Blade Cooling Ducts*, Eindhoven University of Technology.

[6] Adrian Dahlquist, 2008, *Axial Gas Turbine Blade Cooling with Impingement/Film-Cooling*, Lund University

[7] J.C. Han, 2002, Recent Studies in Turbine Blade Cooling, *9th International Symposium on Rotaring Machinery.*

[8] LTT (Laboratoire de Thermique apploquée et de Turbomachines). 1 Jun 2010, http://lttwww.epfl.ch/research/htprojects/filmcool.htm

[9] Martin Oldfield, 15 Sept 2007 http://www.soue.org.uk/souenews/issue7/osney.html

[10] X. Gao & B. Sundén, 15th May 2000, *Heat Transfer Distribution in Rectangular Ducts with V-shaped Ribs*, Heat and Mass Transfer

[11] Fundamental of gas Turbine Engine, http://www.cast-safety.org/pdf/3_engine_fundamentals.pdf

## DIGITIZER

For the turbine blade dimension, the real model is sent to Block 18 for digitizing using a digitizer. By using this digitizer, the real dimension or the outer shape of the blade can be plotted obtained. The design will be in Autocad form. After we get this drawing in Autocad, we can export it to Gambit for simulation using Fluent. SAT Export must be downloaded and installed in order to export the drawing in Autocad to Gambit. The format form used is SAT. Since it is free, the trial software can be used for 10 times or 10 days depend which will end earlier.

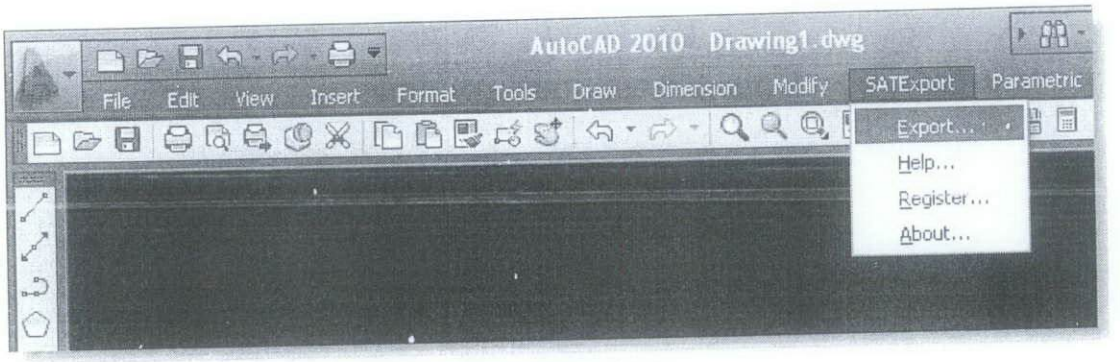


Figure A-1: SAT Export

# APPENDIX B

## USING Gambit

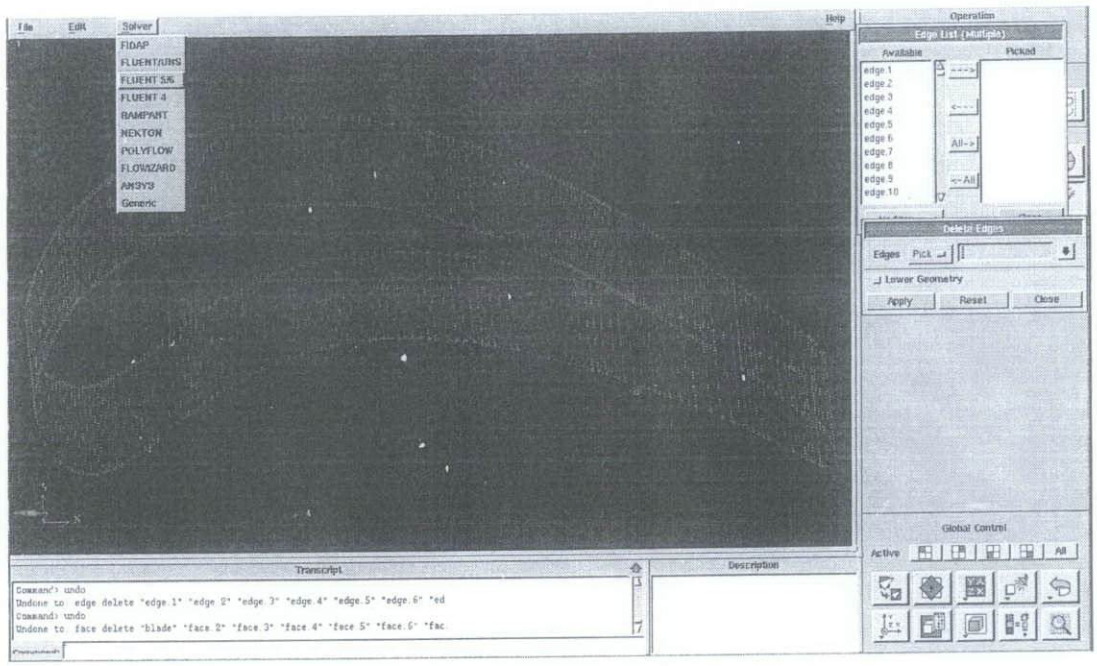


Figure B-1: Selecting solver FLUENT 5/6

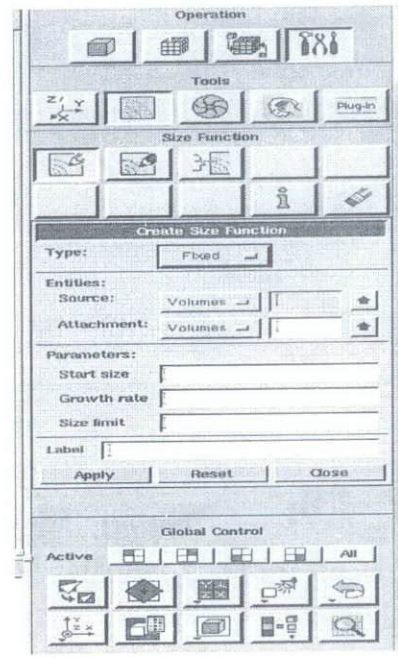


Figure B-2: Setting size function

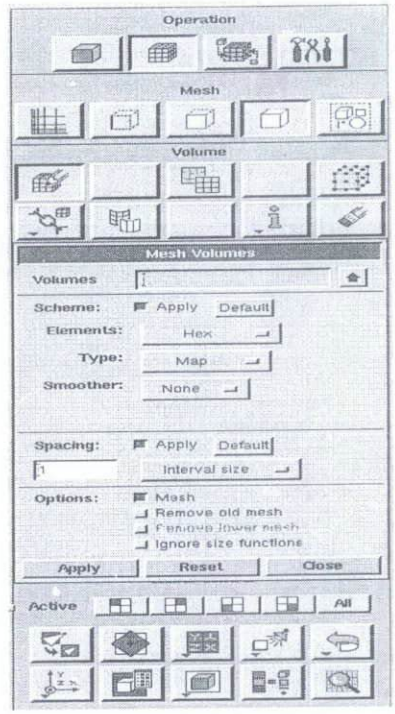


Figure B-3: Meshing the volume of the model

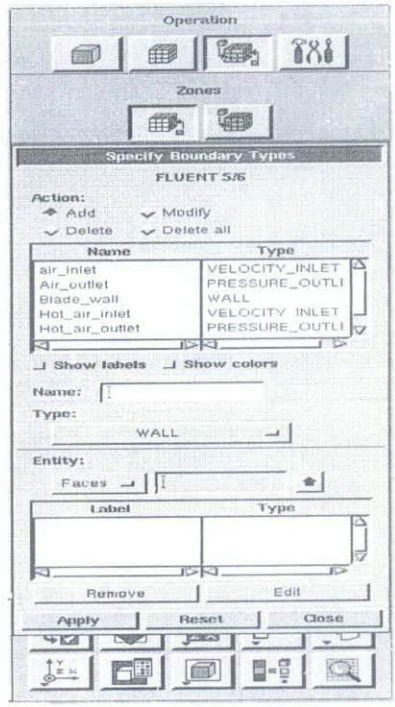


Figure B-4: Setting Boundary Condition

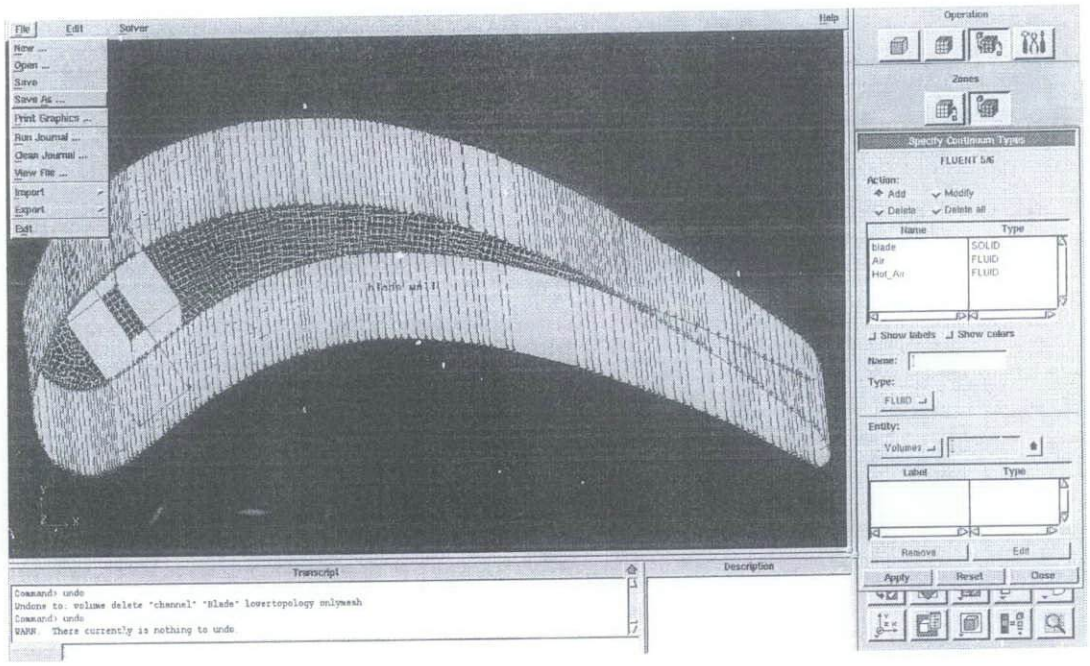


Figure B-5: Saving file

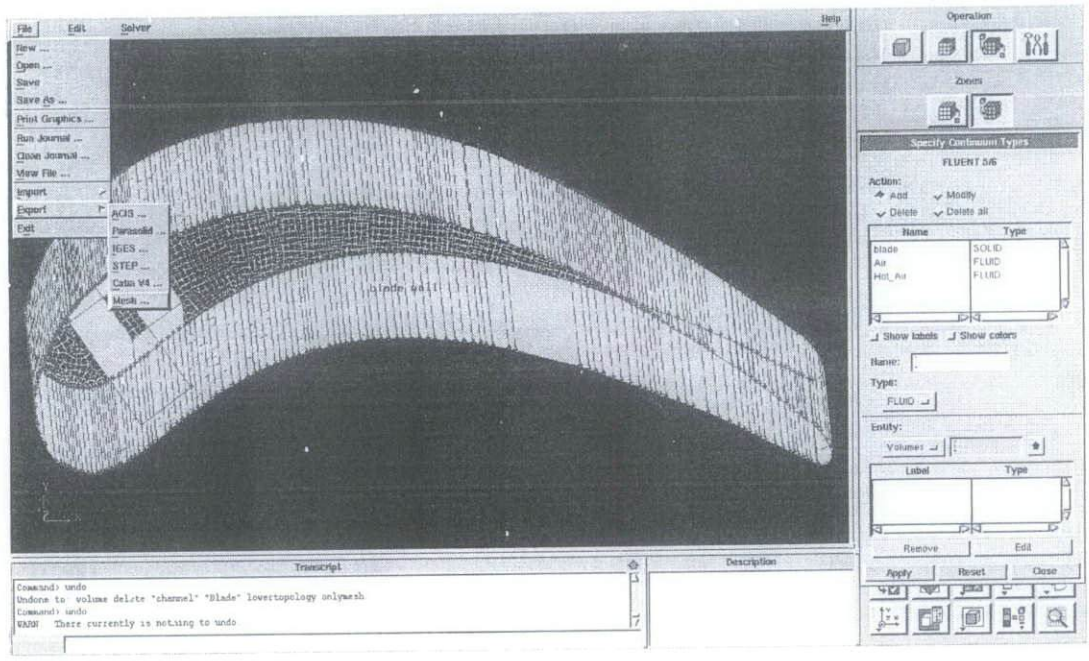


Figure B-6: Exporting 'Mesh' to Fluent

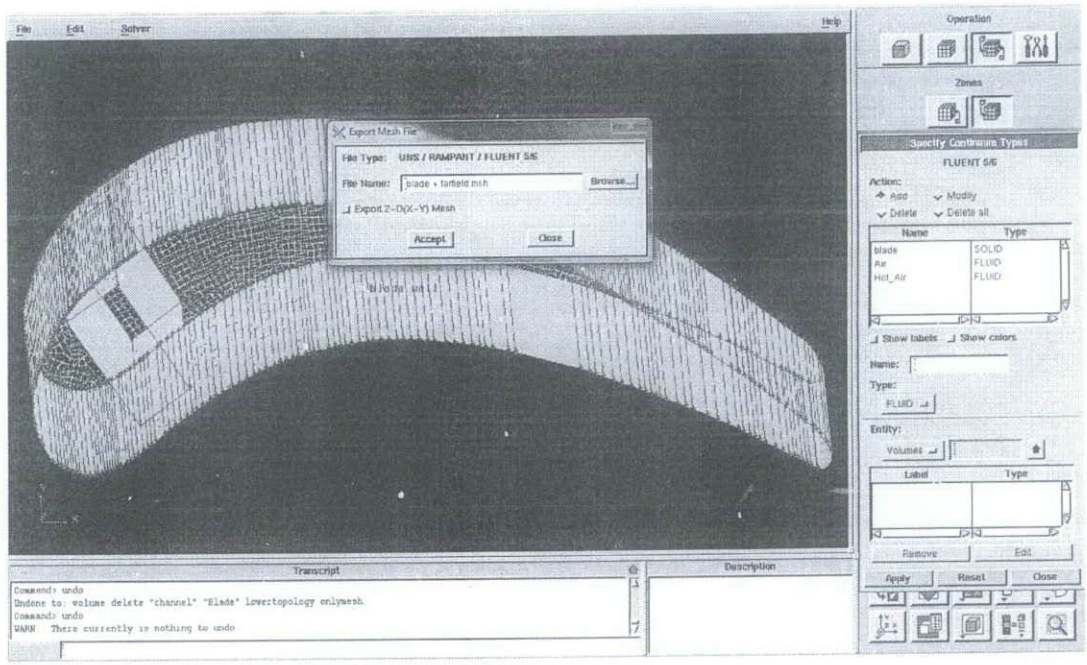


Figure B-7: Do not click 'Export 2D (X-Y) Mesh'

# APPENDIX C

# USING Fluent

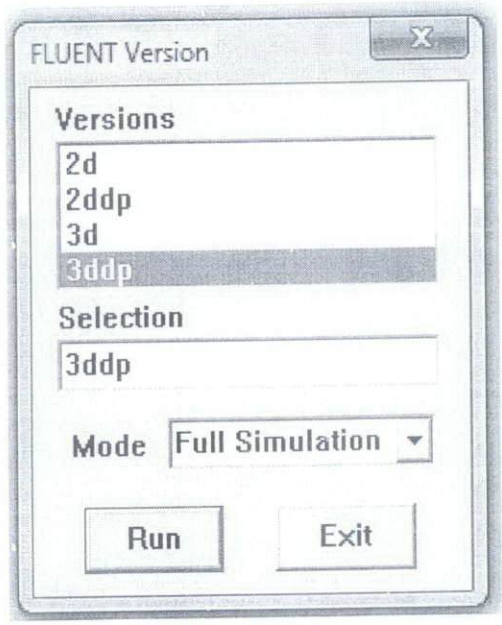


Figure C-1: Select '3ddp' Fluent version

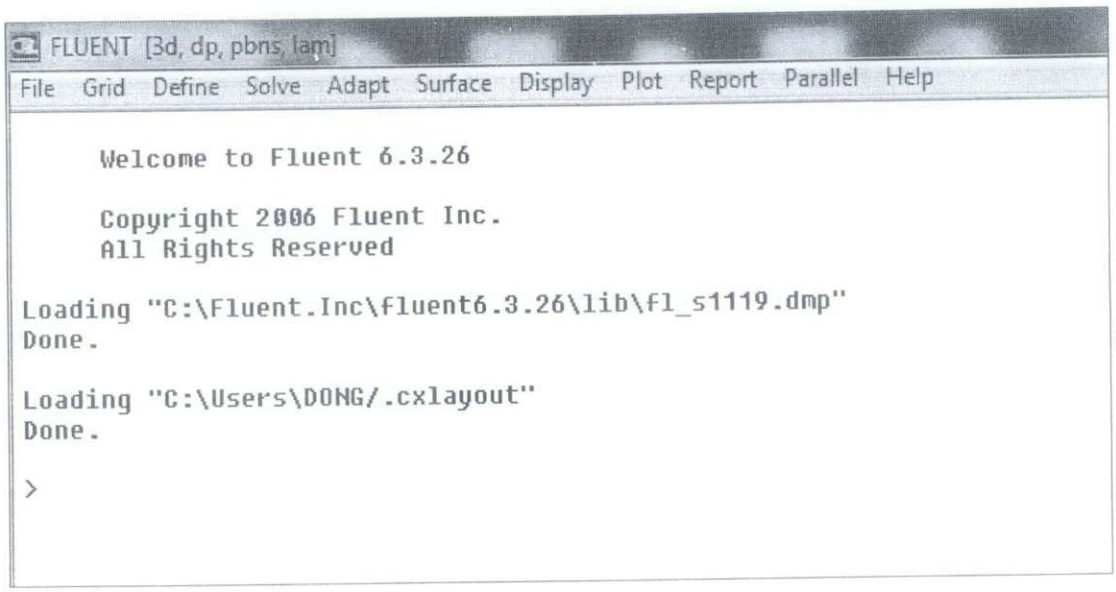


Figure C-2: Fluent layout

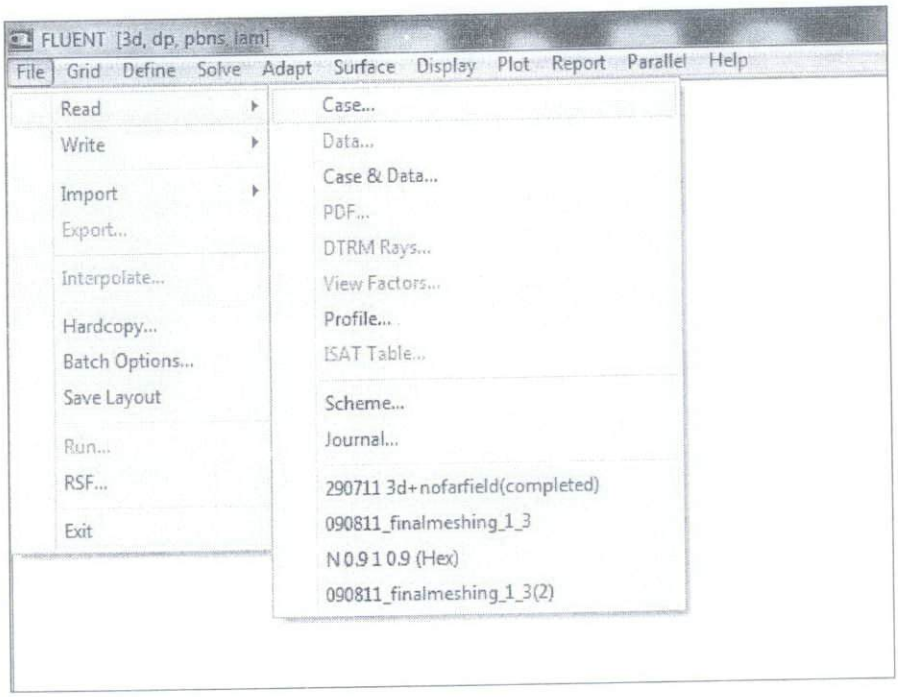


Figure C-3: Select 'Read > Case'

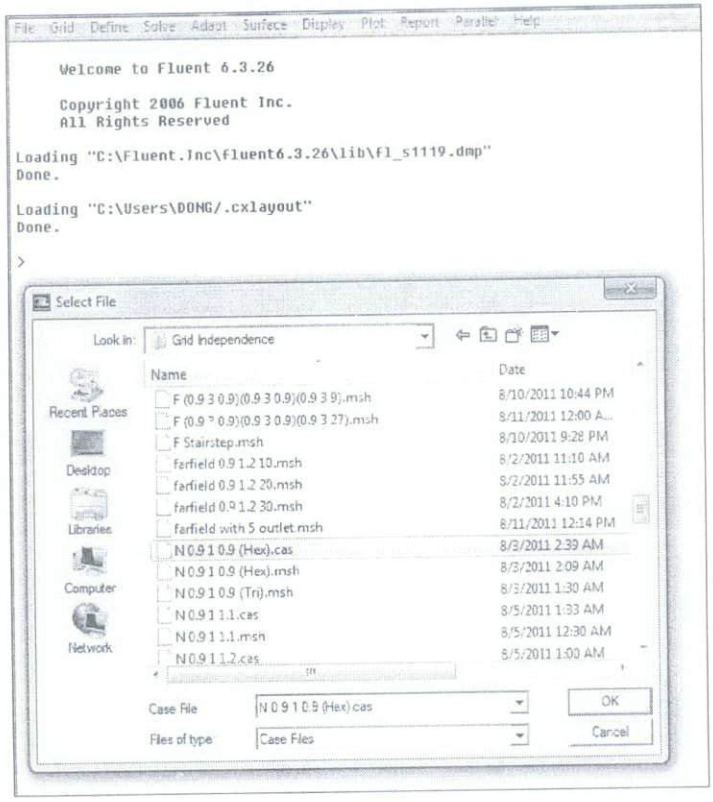


Figure C-4: Select '.msh' from gambit or Select '.cas' for saved data from fluent

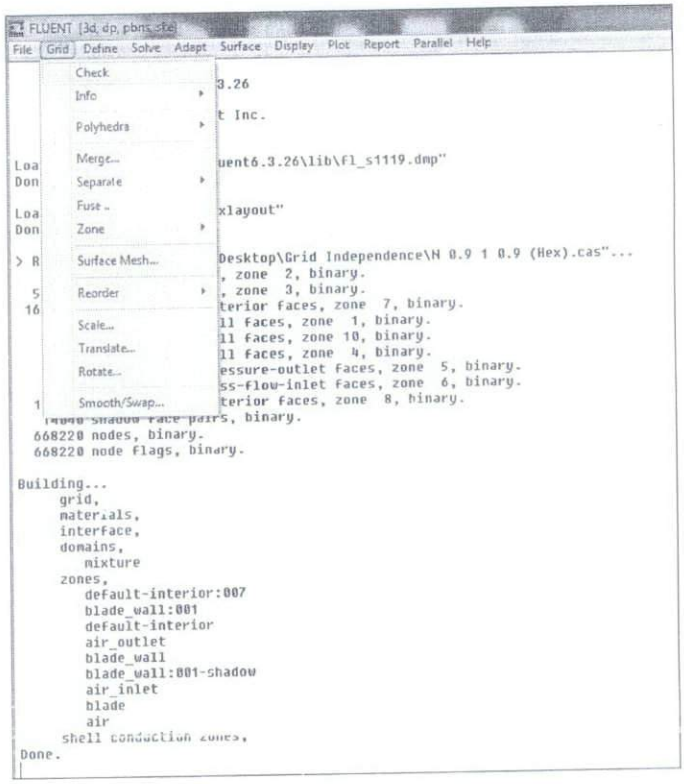


Figure C-5: Click 'Grid > Check'

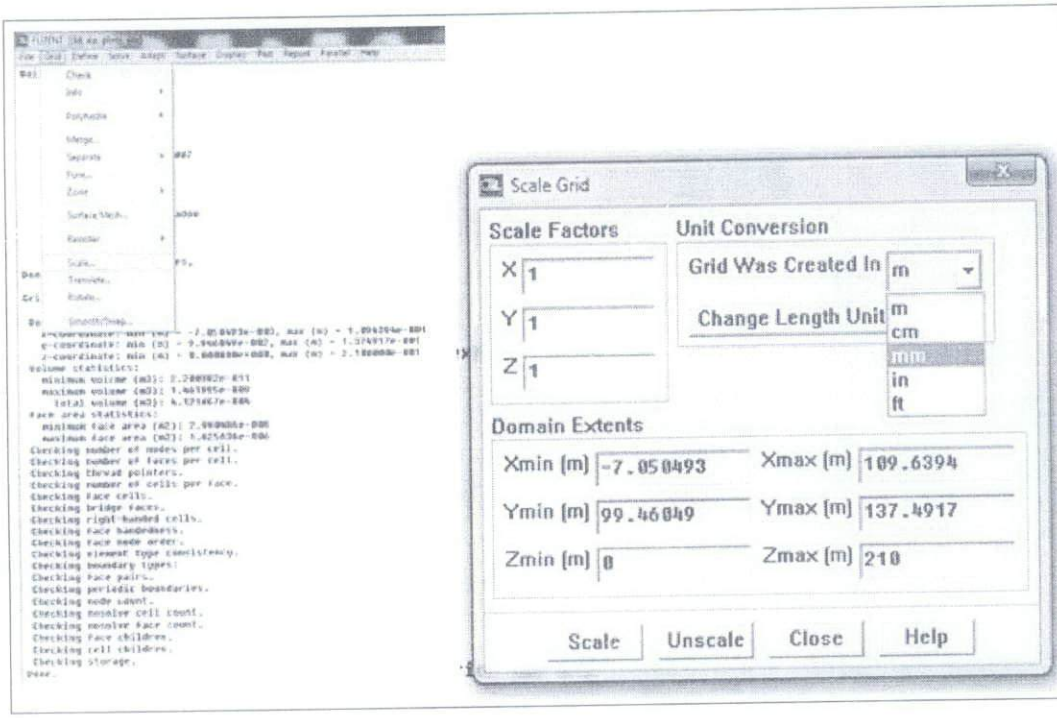


Figure C-6: Click 'Grid > Scale' and change to 'mm'

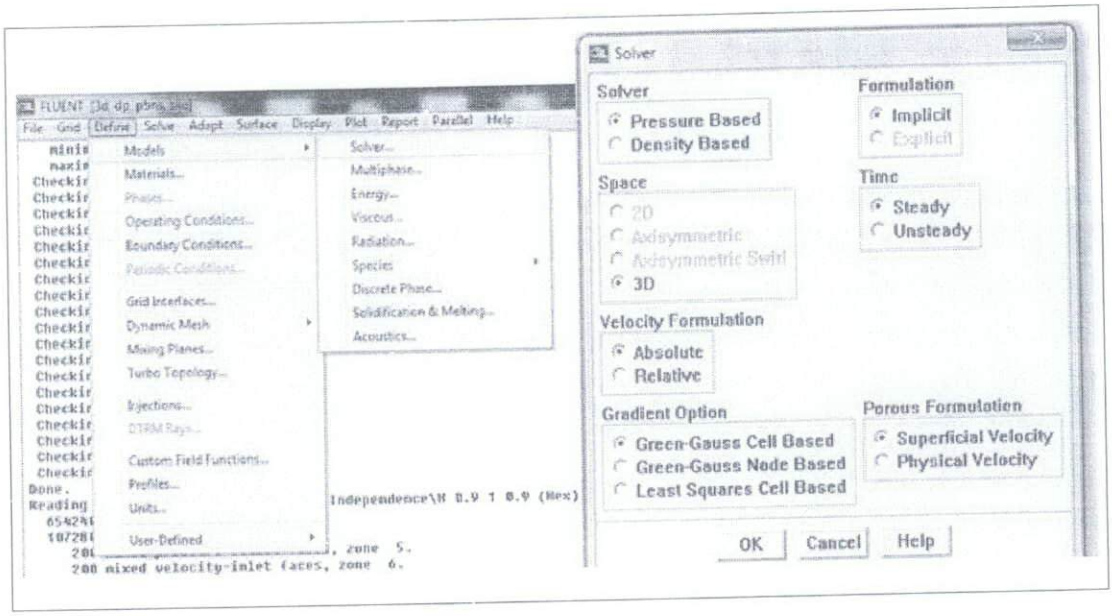


Figure C-7: Select the 'Pressure Based' solver

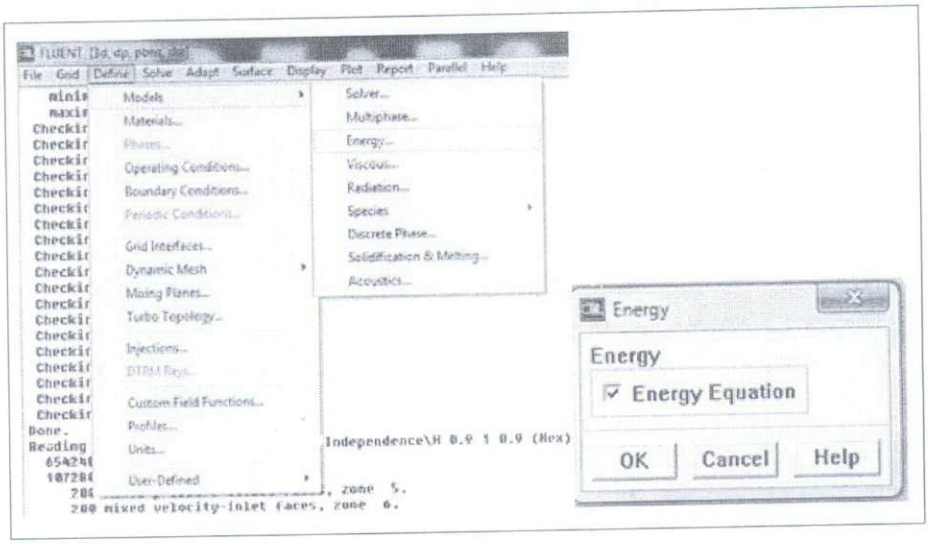


Figure C-8: Click 'Energy Equation'

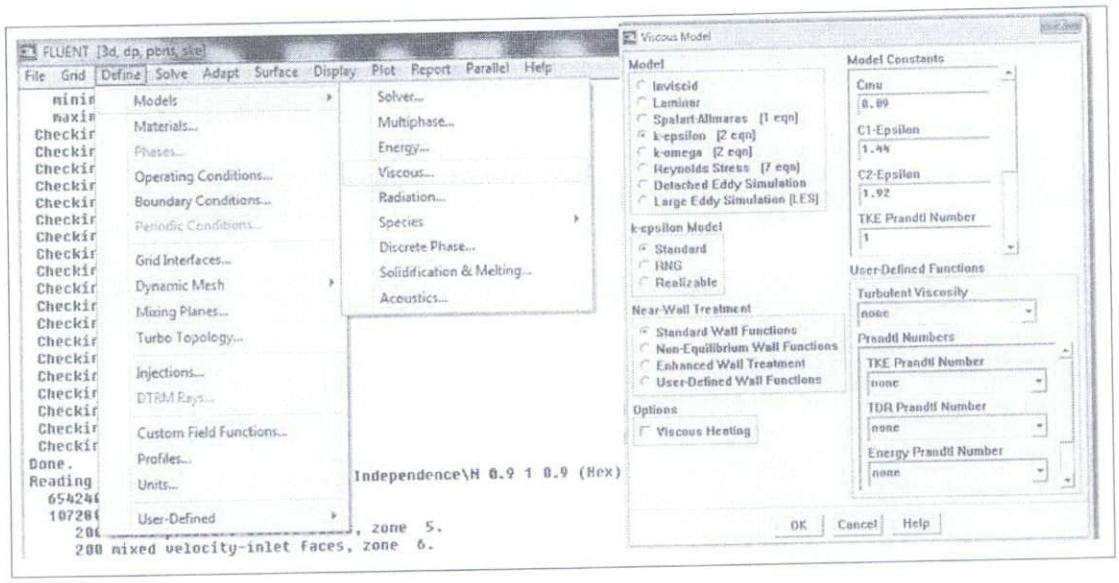


Figure C-9: Select 'k-epsilon' for turbulence flow

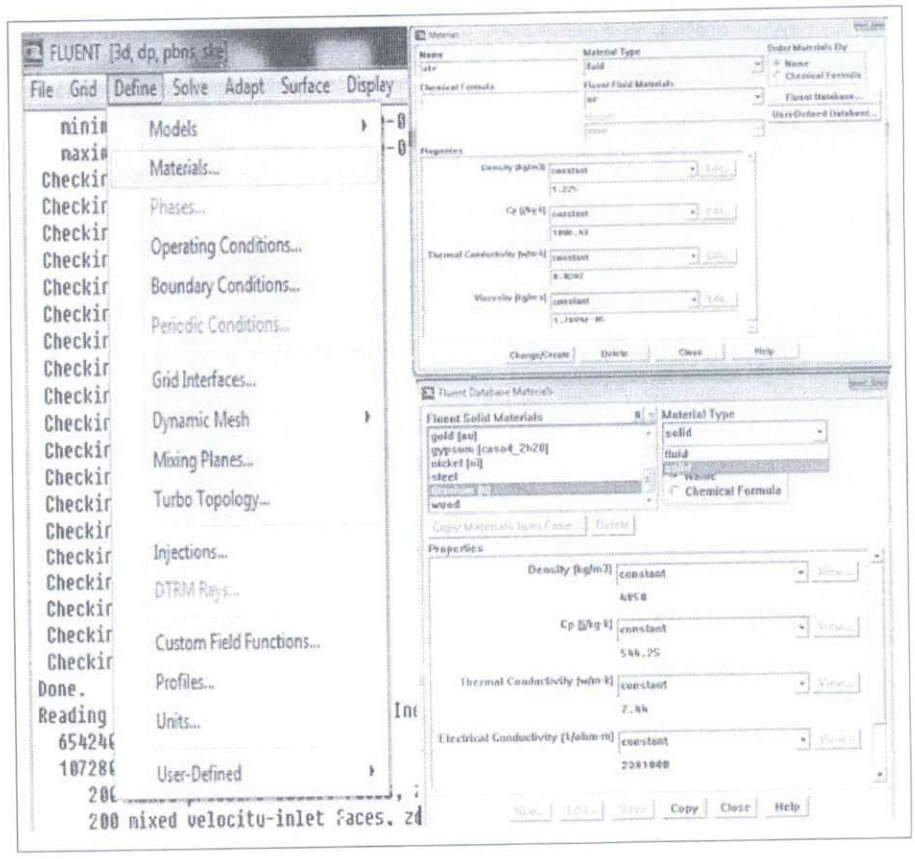


Figure C-10: Select the material

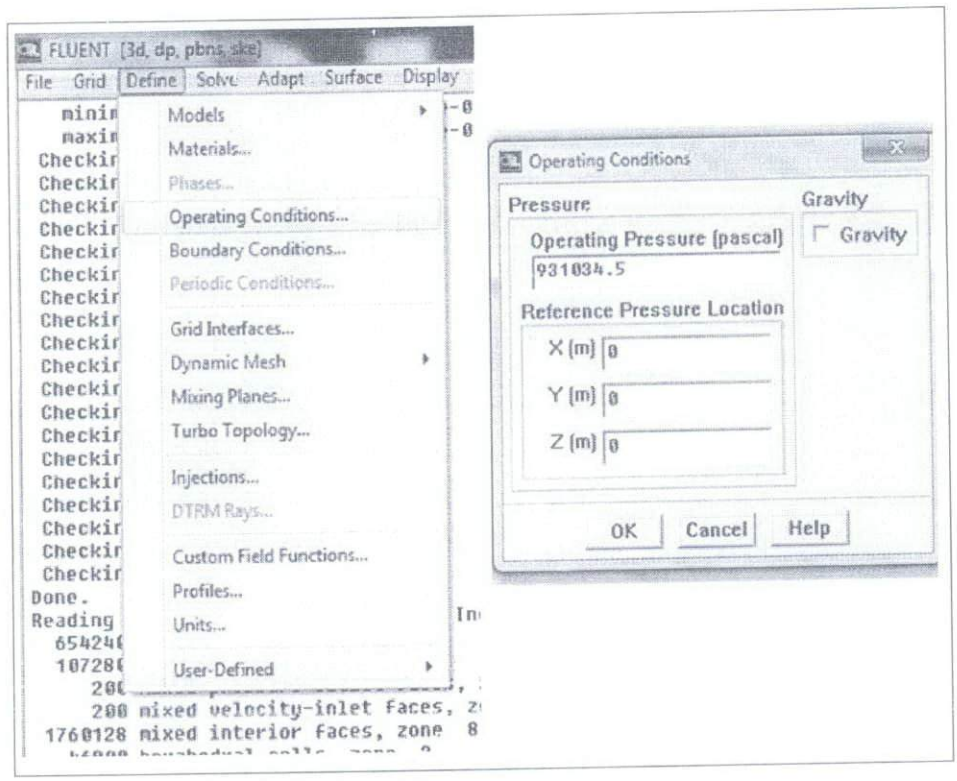


Figure C-11: Set the Operating Pressure

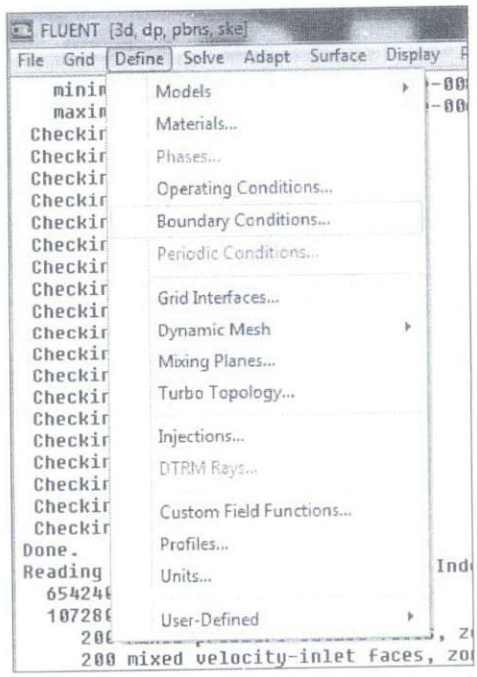


Figure C-12: Click 'Define > Boundary Condition'

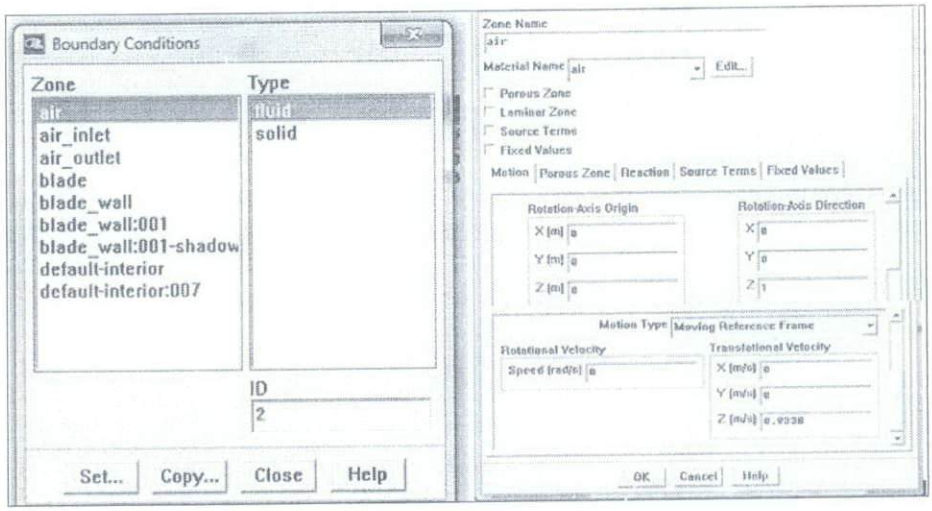


Figure C-13: Setting for 'air'

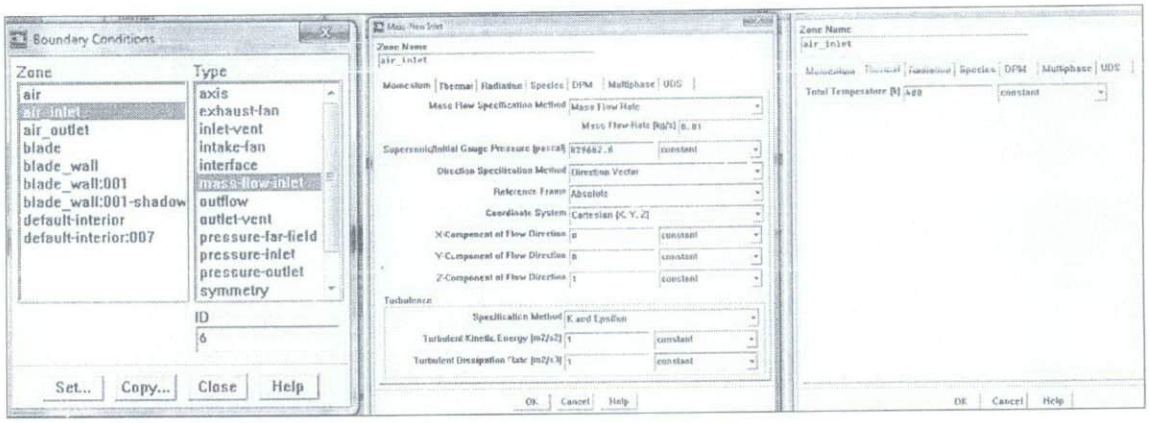


Figure C-14: Setting for 'air_inlet'

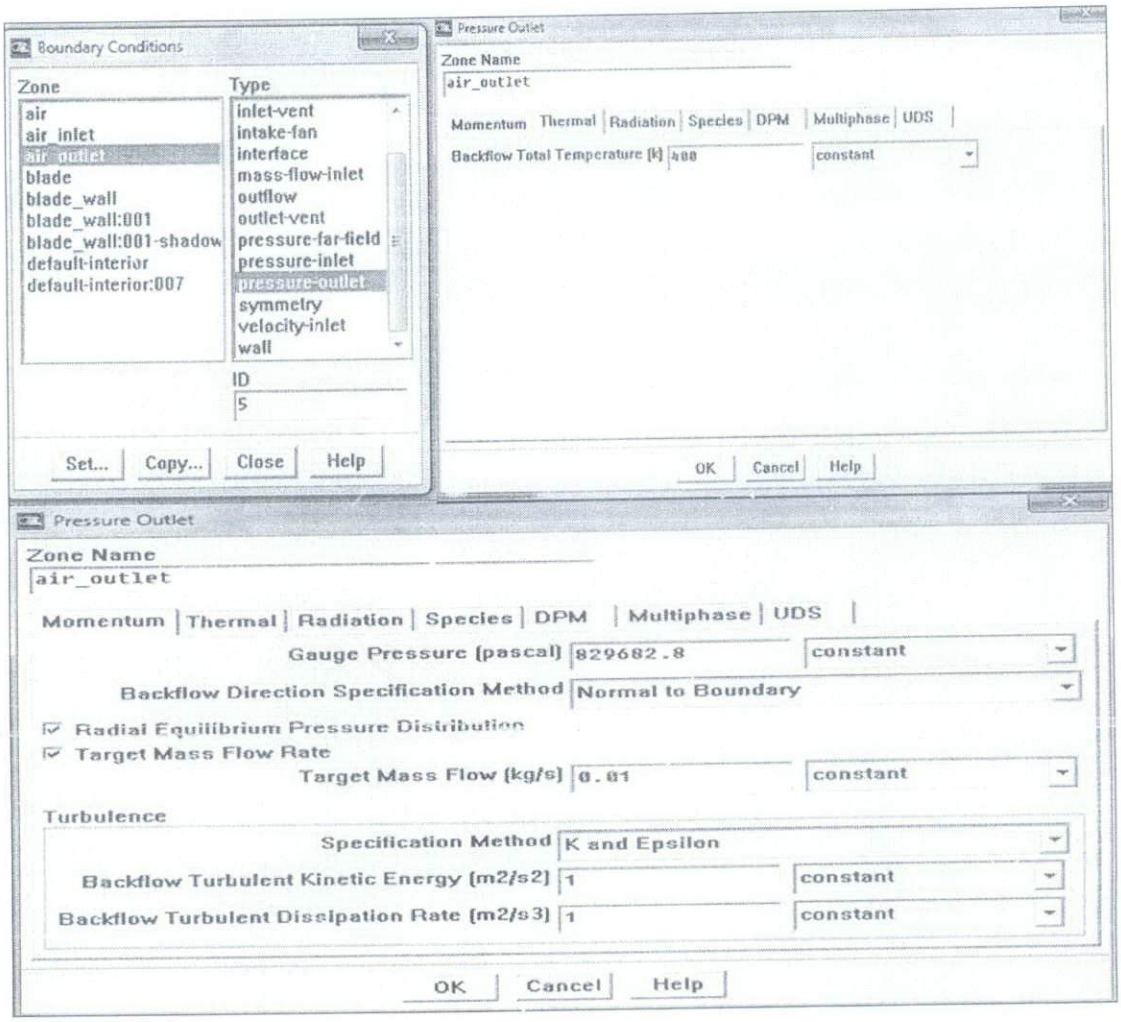


Figure C-15: Setting for 'air_outlet'

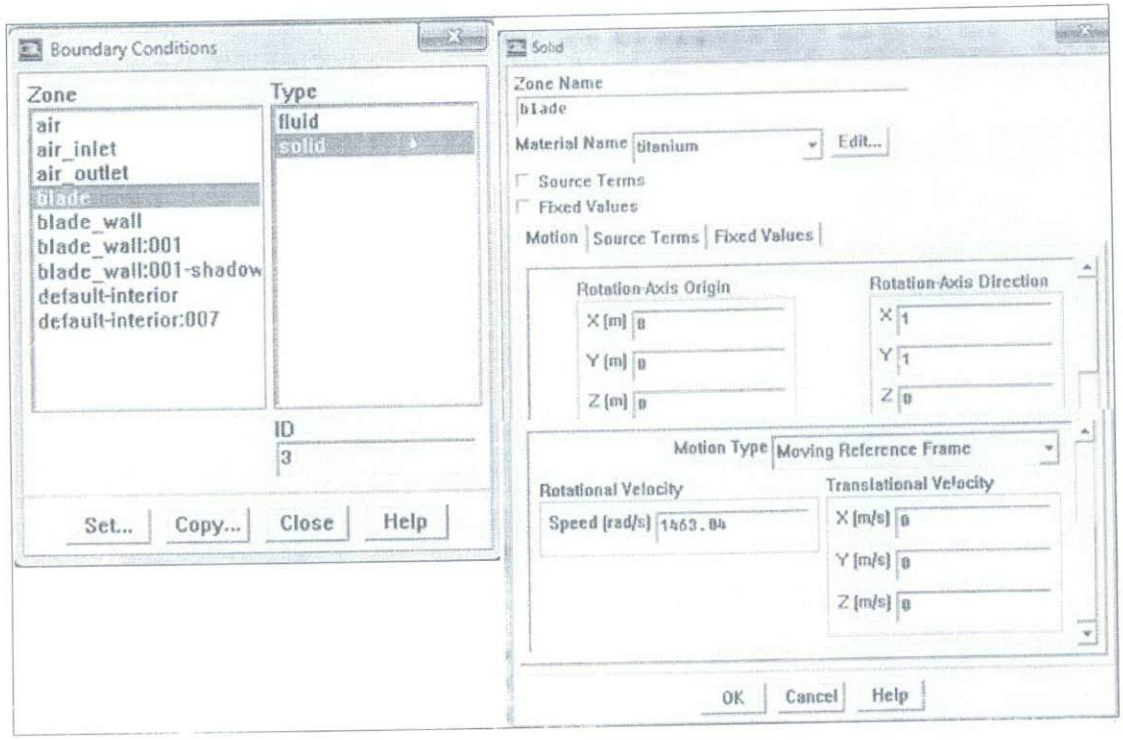


Figure C-16: Setting for 'blade'


Figure C-17: Setting for 'blade_wall'

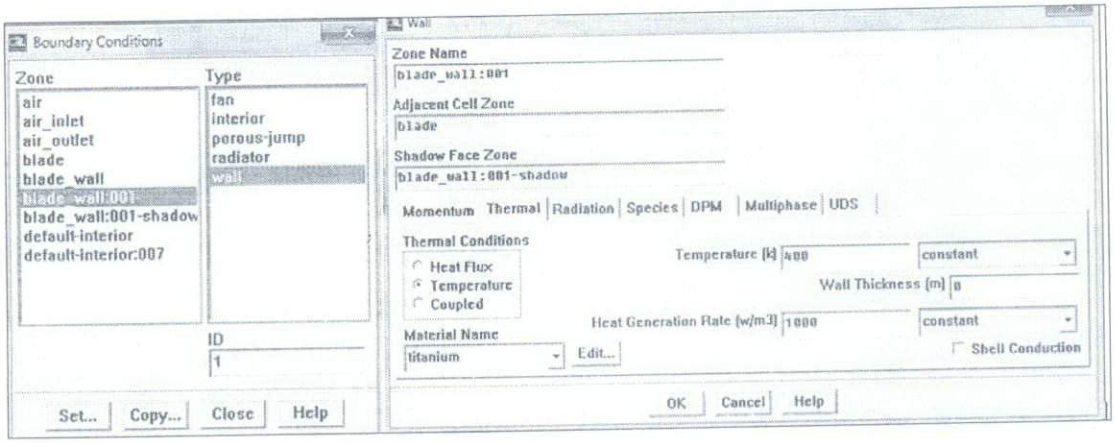


Figure C-18: Setting for 'blade_wall:001'

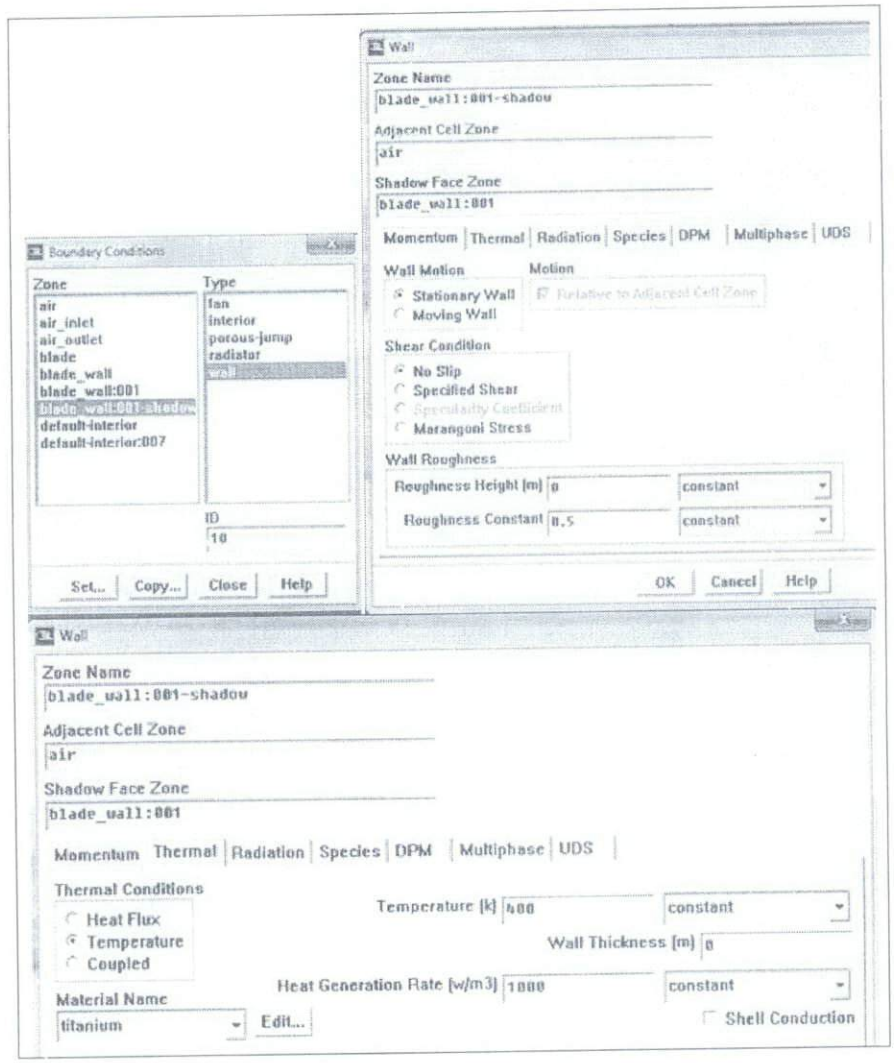


Figure C-19: Setting for 'blade_wall:001-shadow'

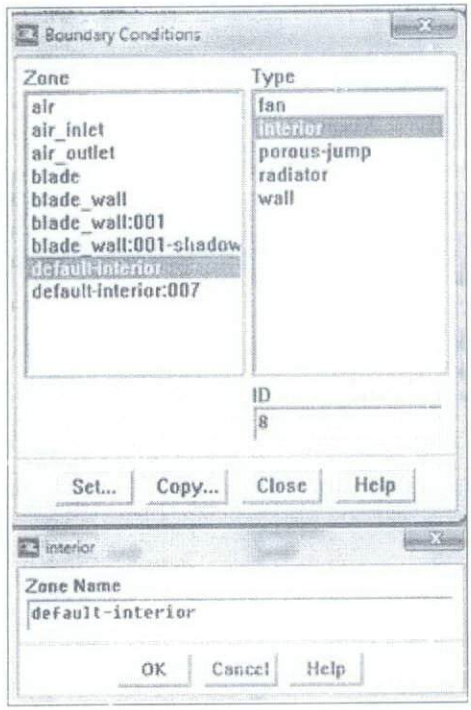


Figure C-20: Setting 'default-interior'

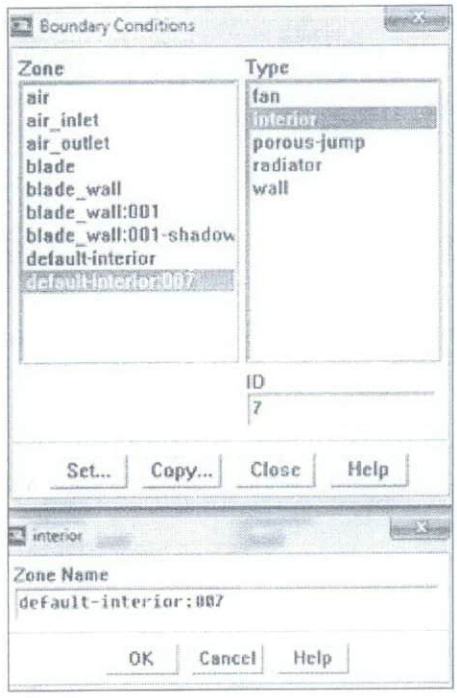


Figure C-21: Setting 'default-interior:007'

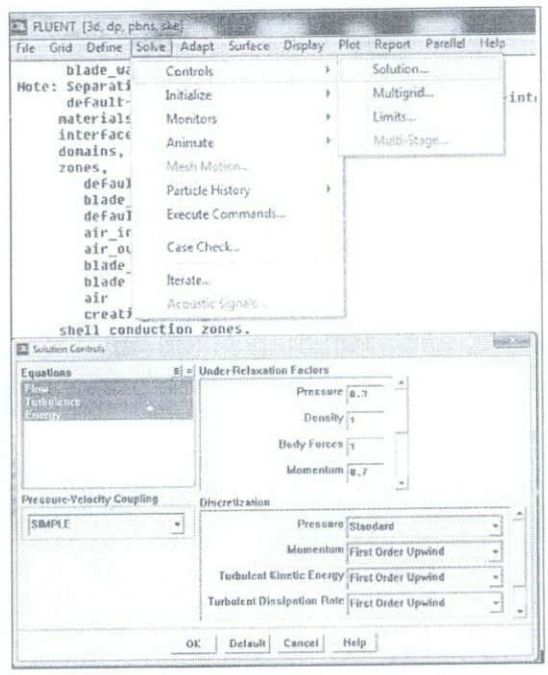


Figure C-22: Choose the solution control

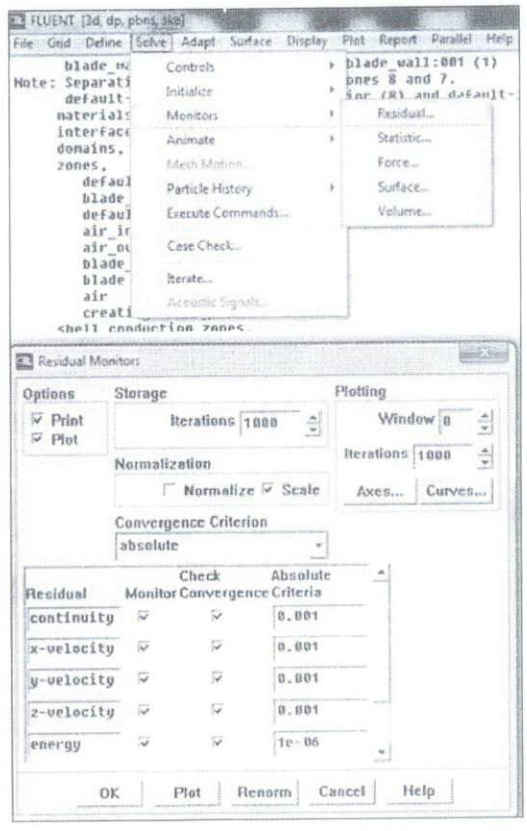


Figure C-23: Click 'Plot' to view the residual

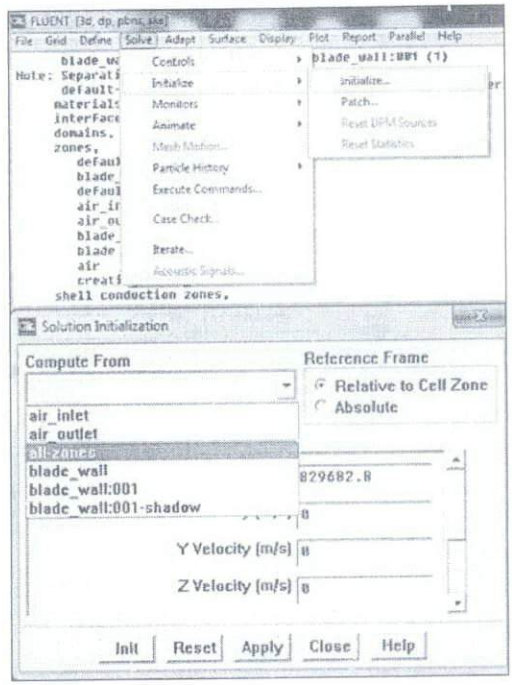


Figure C-24: Click 'Initialze > all-zones'

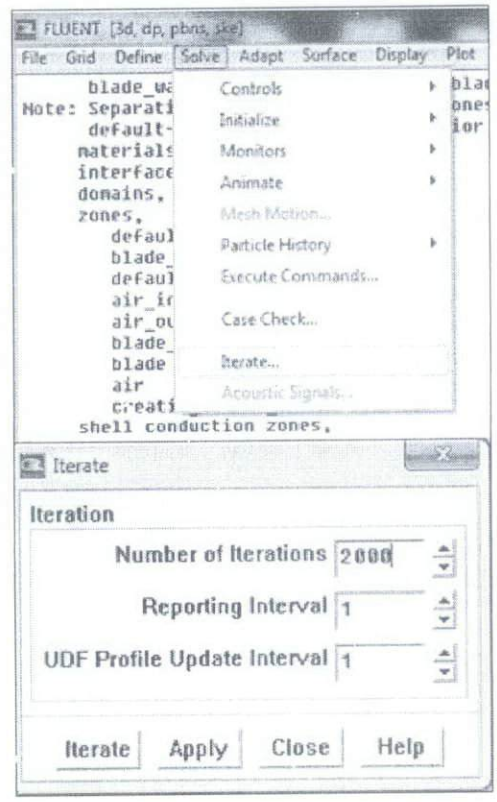


Figure C-25: Iteration is set until the simulation converge

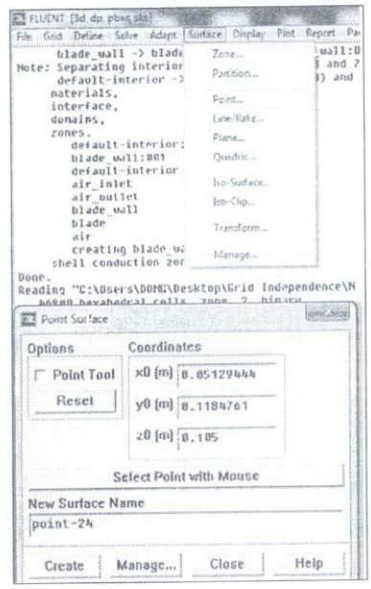


Figure C-26: Set points to be viewed using coordinates

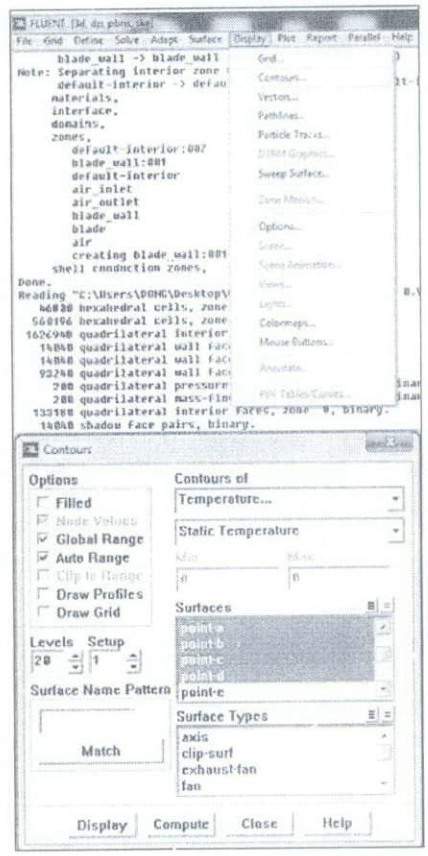


Figure C-27: Select 'Display > Contour' to view the points

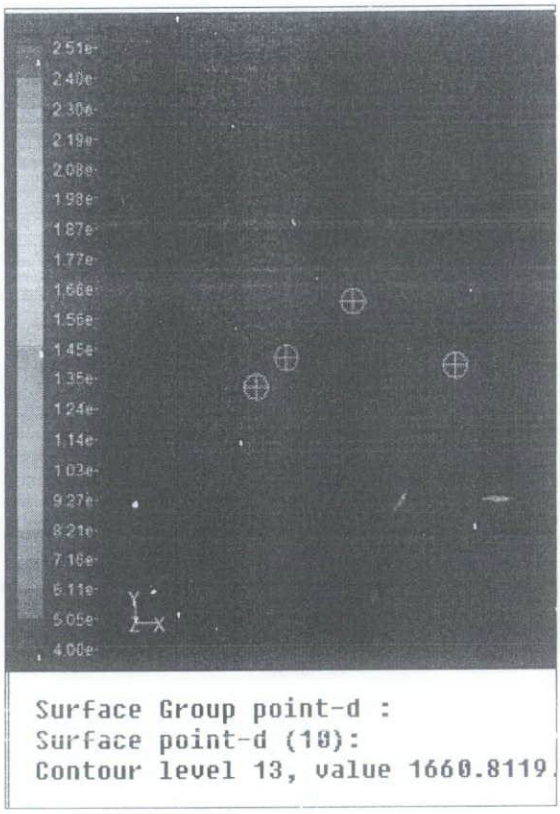


Figure C-28: Right Click the point to get the temperature